

# Battle of the Leakage Detection and Isolation Methods

Stelios G. Vrachimis<sup>1</sup>, Demetrios G. Eliades<sup>2</sup>, Riccardo Taormina<sup>3</sup>, Zoran Kapelan<sup>4</sup>, Avi Ostfeld<sup>5</sup>,  
Shuming Liu<sup>6</sup>, Marios Kyriakou<sup>7</sup>, Pavlos Pavlou<sup>8</sup>, Mengning Qiu<sup>9</sup>, and Marios M. Polycarpou<sup>10</sup>

<sup>1</sup>Postdoctoral Research Associate, KIOS Research and Innovation Center of Excellence,  
Department of Electrical and Computer Engineering, University of Cyprus, Nicosia, Cyprus;  
Email: vrachimis.stelios@ucy.ac.cy

<sup>2</sup>Research Assistant Professor, KIOS Research and Innovation Center of Excellence, University of  
Cyprus, Nicosia, Cyprus; Email: eldemet@ucy.ac.cy

<sup>3</sup>Assistant Professor, Faculty of Civil Engineering and Geosciences, Department of Water  
Management, Delft University of Technology, Stevinweg 1, 2628 CN Delft, Netherlands; E-mail:  
r.taormina@tudelft.nl

<sup>4</sup>Professor, Department of Water Management, Delft University of Technology, Stevinweg 1, 2628  
CN Delft, Netherlands; E-mail: z.kapelan@tudelft.nl

<sup>5</sup>Professor, Faculty of Civil and Environmental Engineering, Technion – Israel Institute of  
Technology, Haifa 32000, Israel; E-mail: ostfeld@tx.technion.ac.il

<sup>6</sup>Professor, School of Environment, Tsinghua University, Beijing 100084, China; Email:  
shumingliu@tsinghua.edu.cn

<sup>7</sup>Research Software Engineer, KIOS Research and Innovation Center of Excellence, University of  
Cyprus, Nicosia, Cyprus; Email: kiriakou.marios@ucy.ac.cy

<sup>8</sup>Research Engineer, KIOS Research and Innovation Center of Excellence, University of Cyprus,  
Nicosia, Cyprus; Email: pavlou.v.pavlos@ucy.ac.cy

<sup>9</sup>Postdoctoral Research Fellow, Faculty of Civil and Environmental Engineering, Technion –  
Israel Institute of Technology, Haifa 32000, Israel; Email: mengning.qiu@campus.technion.ac.il

<sup>10</sup>Professor, KIOS Research and Innovation Center of Excellence, Department of Electrical and  
Computer Engineering, University of Cyprus, Nicosia, Cyprus; Email: mpolycar@ucy.ac.cy

## 26 **ABSTRACT**

27 A key challenge in designing algorithms for leakage detection and isolation in drinking water  
28 distribution systems, is the performance evaluation and comparison between methodologies using  
29 benchmarks. For this purpose, the “Battle of the Leakage Detection and Isolation Methods” (Bat-  
30 tLeDIM) competition was organized in 2020 with the aim to objectively compare the performance  
31 of methods for the detection and localization of leakage events, relying on SCADA measurements  
32 of flow and pressure sensors installed within a virtual water distribution system. Several teams from  
33 academia and the industry submitted their solutions, using various techniques including time-series  
34 analysis, statistical methods, machine learning, mathematical programming, meta-heuristics and  
35 engineering judgment, and were evaluated using realistic economic criteria. This paper summa-  
36 rizes the results of the competition and conducts an analysis of the different leakage detection  
37 and isolation methods used by the teams. The competition results highlight the need for further  
38 development of methods for leakage detection and isolation, and also the need to develop additional  
39 open benchmark problems for this purpose.

## 40 **INTRODUCTION**

41 Drinking Water Distribution Networks (DWDN) are susceptible to infrastructure failures, which  
42 may lead to water losses. The global average Non-Revenue Water (NRW) is 30%, with an estimated  
43 annual cost of \$39 billion USD (Liemberger and Wyatt 2019). A significant part of NRW is due to  
44 background leakages and pipe bursts, which may occur anywhere within the distribution network.  
45 Background leakages are typically difficult to detect due to their small size, whereas pipe bursts  
46 are easier to locate as they are of larger size and may appear on the surface. The early detection  
47 and localization of any leakage event is crucial, as this reduces the time required for addressing the  
48 event and therefore reducing the risk of further infrastructure degradation, contamination events  
49 and consumer complaints.

50 Leakage diagnosis in water distribution systems has attracted a great deal of attention from both  
51 practitioners and researchers over the past years (Chan et al. 2018). The process of leakage diagnosis  
52 can be separated into: leakage detection, which focuses on identifying the existence of a leak in the

53 network; and leakage localization, which aims to provide an approximate location of leakages given  
54 the available measurements. A recent review paper (Chan et al. 2018) classifies leakage detection  
55 methodologies into Passive and Active methods. Passive methods (also referred to as equipment-  
56 based, hardware or external methods) require the deployment of specialized equipment, such as  
57 acoustic sensors or ground penetrating radars, at areas that are suspect of leakage. Active methods  
58 (also referred to as internal or software methods) are methods that are based on the presence of  
59 permanently installed sensors which continuously monitor the system for leakages. The latest  
60 developments in hydraulic sensor technology and on-line data acquisition systems have enabled  
61 water companies to deploy a larger number of more accurate pressure and flow devices with less  
62 cost. These data can be used to monitor the system in real-time and develop methodologies that use  
63 the data to detect and pre-localize leaks using Active methods. Pre-localization is the process of  
64 defining an area in which the leak exists, instead of pin-pointing exactly its location. This research  
65 area has witnessed a significant interest, as indicated in recent review papers (Li et al. 2015; Chan  
66 et al. 2018; Zaman et al. 2019).

67 The term *model-based leakage diagnosis* is used to describe methodologies that utilize a model  
68 of the DWDN (also referred to as numerical model) and sensor measurements to estimate the steady-  
69 state hydraulic conditions in the network (Vrachimis et al. 2018b). The operating principle behind  
70 model-based leakage detection, as suggested by (Pudar and Liggett 1992), is to find discrepancies of  
71 measurements to their estimates obtained by the network model, which would indicate the existence  
72 of a leakage. Typically, model-based methods utilize a larger number of pressure sensors than flow  
73 sensors because they are cheaper and easier to install and maintain (Pérez et al. 2011). However,  
74 DWDN are large-scale systems and the number of sensors used in practice is still small compared  
75 to the system size. Moreover, to enhance leakage diagnosis, methodologies for optimal placement  
76 of pressure sensors are used (Farley et al. 2010; Casillas et al. 2013; Cuguero-Escofet et al. 2017).  
77 Finally, the consideration of measurement and model uncertainties is important when using these  
78 methods to determine if the network is operating in a normal state (Vrachimis et al. 2019) and  
79 should be taken into account before making a decision about the occurrence of a leakage in the

80 network (Vrachimis et al. 2018a).

81 Leakage localization methods are typically model-based due to the limited information provided  
82 by the small number of sensors; one of the first representative examples is the work in (Wu et al.  
83 2009) where the authors develop a model-based approach for leak localization which is applied to  
84 a large real system. Another interesting model-based approach applied on real systems is found  
85 in (Sophocleous et al. 2019), where the authors formulate an optimization problem to perform  
86 leakage diagnosis and deal with the dimensionality of the problem using search space reduction to  
87 reduce decision variables. Some approaches relate the acquired measurements with the simulated  
88 output from many simulated leakage scenarios on different locations of the network (Farley et al.  
89 2010; Goulet et al. 2013); the geographical mapping of each model component can then be used  
90 to indicate the probability that a zone contains a leakage (Perez et al. 2014). Researchers have  
91 also used pressure residual analysis, by creating a system pressure sensitivity matrix to identify the  
92 location of leaks, based on the assumption of a single leakage occurring in the system (Pérez et al.  
93 2011; Cuguero-Escofet et al. 2017). A more recent approach considers modeling uncertainties  
94 to create a set-bounded model of the system and then incorporates sensor measurements in an  
95 optimization-based framework to detect and pre-localize leakages using the concept of model-  
96 invalidation (Vrachimis et al. 2021).

97 Data-driven methods (also referred to as non-numerical model methods) do not require a model  
98 to perform detection. Leakage detection methodologies typically follow a data-driven approach; the  
99 authors in (Wu and He 2021) provide the latest review on this topic, and present a practical approach  
100 for anomaly event detection (including but not limited to leaks), classification and evaluation. Some  
101 approaches may require large amounts of reliable training data where the events are labeled by the  
102 operators or experts and they may perform poorly when data is not available (Li et al. 2015). An  
103 example of a data-driven approach is found in (Mounce et al. 2002) where the authors introduced  
104 artificial neural networks (ANNs) for burst detection and have continued to extend their work in the  
105 following years (Mounce et al. 2010). Another approach is found in (Eliades and Polycarpou 2012)  
106 where the authors proposed an algorithm which analyzes the discrete inflow signal of a District

107 Metered Area (DMA) by using an adaptive approximation methodology for updating the coefficients  
108 of a Fourier series and detects leakages by utilizing the Cumulative Sum (CUSUM) algorithm. The  
109 authors in (Soldevila et al. 2016) used a mixed model-based and data driven approach to improve  
110 performance. The study in (Wu and Liu 2017) provides a review on data-driven approaches for  
111 burst detection. The study concludes that these approaches are promising for use in real-life burst  
112 detection, however, reducing false alarms is still an important issue. Moreover, a comprehensive  
113 performance evaluation procedure, especially under different network configurations, might be  
114 necessary.

115 Leakage diagnosis methods are commonly evaluated on private commercial datasets (Chan et al.  
116 2018), and as a result, it is not possible to objectively compare different methods in their ability to  
117 detect and isolate leaks. Moreover, data from real systems may not be readily available, while many  
118 aspects of the system operation are unknown. For example, information about the exact location,  
119 magnitude and time profile of leakages are typically unknown, but crucial when evaluating leakage  
120 diagnosis methodologies. The middle ground between evaluating algorithms on real systems and  
121 having all the available information about the system, is the development of a realistic simulation  
122 benchmark, built upon the expertise of practitioners, of which the operation resembles that of a  
123 real system. Recently, a benchmark leakage detection dataset has been developed named LeakDB  
124 (Vrachimis et al. 2018c), created using the WNTR tool (Klise et al. 2017). The dataset comprises of  
125 data generated from benchmark networks and uses pressure-driven demands and realistic leakage  
126 modelling (van Zyl et al. 2017). In this work, a realistic open benchmark for leakage detection and  
127 localization is developed and used in a “battle” (Taormina et al. 2018), to allow different teams to  
128 evaluate their methods in a unified way.

129 The *Battle of Leakage Detection and Isolation Methods* (BattLeDIM), was organized in 2020  
130 initially as part of the CCWI/WDSA 2020 conference (the conference was postponed due to the  
131 COVID-19 pandemic). The competition aimed to objectively compare the performance of methods  
132 for the detection and localization of leakage events, relying on SCADA measurements of flow and  
133 pressure sensors generated using a realistic virtual city, which was based on a real water distribution

134 network in Cyprus. The overall objective was to detect as many leakages as possible, as fast as  
135 possible and as close to the source as possible, while avoiding false alarms. Participants could use  
136 different types of tools and methods, including (but not limited to) engineering judgement, machine  
137 learning, statistical methods, signal processing, and model-based fault diagnosis approaches. In  
138 total, 18 teams from universities and industry around the world have submitted their solutions to  
139 the competition, and the results were presented on an online workshop organized on September 3,  
140 2020.

141 The main contributions of this work are: 1) introduce a new benchmark network named “L-  
142 Town”, developed for the purposes of the competition, along with a benchmark SCADA dataset;  
143 2) provide an overview of the different leakage and isolation methodologies presented at the  
144 BattLeDIM competition and 3) analyze their results with respect to different objectives by proposing  
145 a comprehensive evaluation procedure.

## 146 **THE L-TOWN BENCHMARK NETWORK**

147 Below we introduce a new benchmark water distribution network, which we refer to as “L-  
148 Town”. This is a city-scale model inspired by a coastal city in Cyprus, which can be used for  
149 research purposes. The network has been suitably modified and redesigned for security purposes.  
150 The L-Town is part of the *KIOS Virtual City Testbed*, an open software platform for simulating the  
151 SCADA operation of different critical infrastructures, including water, power, telecommunications  
152 and transportation systems.

### 153 **Topology and structure**

154 The L-Town model, depicted in Fig. 1, is represented using the EPANET input file format.  
155 It has 782 junctions and 905 pipe segments of approximately 50 meters length each and delivers  
156 drinking water to around 10,000 consumers and industries. It comprises of a network of steel pipes  
157 with a total length of 42.6 km and roughness coefficients (C values) between 120-140. The L-Town  
158 network has a *loop ratio* of 25%, a measure of complexity when solving the hydraulics of the  
159 network; it indicates that 25% of the pipes have to be removed in order to eliminate all loops from

160 the network (Vrachimis et al. 2019). The node elevations range between 1.5 m and 75 m above the  
161 sea level.

162 The water distribution network of L-Town is receiving water from two reservoirs, and it has been  
163 designed to provide pressure head of at least 20m to all of its consumers. The normal operating  
164 pressure in the network ranges between 20-30 meters. A Pressure Reduction Valve (PRV) is  
165 installed at the lower part of the town (“Area B”), to help reduce background leakages. The network  
166 has different pressure areas, and therefore exhibits different sensitivity to leakages. PRVs are also  
167 installed downstream of the two main reservoirs, to help regulate the pressure. A pump and a water  
168 tank have been installed in the higher part of the town (“Area C”), to provide sufficient pressure to  
169 the consumers of that area. The tank has a diameter of 16 meters with a cylindrical shape. The  
170 pump has been programmed so that the tank refills during the night and empties to “Area C” during  
171 the day.

172 Note that the design decision to include pipes of 50 meters length is based on the following  
173 considerations: First, it is common for a real network to have consumer demand locations at a 50  
174 meter interval, thus, in this sense, the provided benchmark can be considered a detailed version  
175 of a real network. Moreover, for the purposes of this competition, it is more efficient to allow  
176 participants to define a labeled pipe segment when localizing a leak, instead of defining a long  
177 pipe and the position of the leak on that pipe. Finally, the participating teams can apply model  
178 reduction techniques to reduce the complexity of the model and computational cost. This approach  
179 has the benefit of allowing teams to showcase the ability of their methodology to deal with complex  
180 network models. This would not have been possible if a reduced model of the benchmark network  
181 was already provided.

## 182 **Water demand modelling**

183 L-Town is assumed to be located in the Northern hemisphere, thus higher water usage is  
184 expected around July/August, and lower in December/January. No significant variations of water  
185 consumption is observed during holidays or other special days. During workdays (Monday to  
186 Friday), water consumption follows a similar pattern, whereas during the weekend (Saturday and

187 Sunday), there is higher consumption during late hours as the result of night life. Areas with  
188 industrial users do not follow the same pattern of consumption.

189 For constructing the benchmark model, open geospatial data were considered corresponding to  
190 the buildings of the actual location. A clustering algorithm was implemented in QGIS (QGIS.org  
191 2020) to assign each building to a network node, and the node population was assigned to be  
192 proportional to the building area. This was computed using:

$$193 \quad d_i^b = \sum_{j=1}^n (\alpha_i^j \beta_i^j) \gamma_i, \quad (1)$$

194 where  $d_i^b$  is the base demand of node  $i$ ,  $n$  is the number of consumer types,  $\alpha_i^j$  is the percentage  
195 of the  $j$ -th consumer type at the  $i$ -th node,  $\beta_i^j$  the average amount of water consumed in  $m^3/h$  for  
196 each  $m^2$  of a building, and  $\gamma_i$  the total building area corresponding to node  $i$ . In this benchmark,  
197 three types of consumers ( $n = 3$ ) were considered: *residential*, *commercial* and *industrial*.

198 Each node has a unique demand pattern for each consumer type, based on the statistical  
199 characteristics of real metered data from the area. Specifically, a Fourier Series model was used to  
200 approximate the demands (Vrachimis et al. 2018c), capturing seasonality (weekly, yearly) as well  
201 as the uncertainties on demand patterns (see Fig. 2). The overall water consumption is the linear  
202 combination of the base demands with the corresponding patterns.

203 The demand peaking factor, which is the ratio of the Maximum Daily Demand (MDD) to the  
204 Average Daily Demand (ADD) in a water system, was also considered in the design of demand  
205 patterns. The ratio, based on observations from real systems, typically ranges from 1.2 for very  
206 large water systems, to 3.0 or even higher for specific small systems. The demand peaking factor  
207 in L-Town ranges between 1.5 and 2.0, given it is an average size system.

## 208 THE BATTLEDIM CHALLENGE SCENARIO

209 As part of the “Battle of the Leakage Detection and Isolation Methods”, all participating teams  
210 were given the following artificial scenario to establish the challenge:

211 “In previous years, the utility of L-Town was experiencing a large number of pipe breaks and



212 water losses, affecting its service quality. During 2018, a number of leakage events occurred,  
213 which were detected and fixed by the water utility. However, it is believed that a number of smaller  
214 leakages occurred but not revealed. It is also assumed that some leakages occurred abruptly,  
215 whereas others developed gradually, as incipient events, from background leaks into pipe bursts.

216 To assist the L-Town water utility decision-making process, the utility developed an EPANET-  
217 based nominal model of the distribution network, in which base demands were assigned to nodes,  
218 following historical billing data of proximity consumers. Moreover, two nominal demand patterns  
219 were identified for residential and commercial consumer types (with some discrepancies). The  
220 utility believes that there might be some inaccuracies in the model, e.g., with respect to the pipe  
221 roughness and pipe diameters. In addition, the utility was not able to confirm the status of all the  
222 valves in the network (i.e., whether they are open or closed).

223 The L-Town water utility is searching for a solution to help them analyze the SCADA dataset,  
224 and detect leakage events as fast as possible. In addition, it is crucial for the utility to have an  
225 indication where approximately the leakage occurs, so that the field workers can inspect those  
226 potential leaks using their equipment.

227 The L-Town utility has created an open call for teams to demonstrate their ability in detecting and  
228 localizing leakage events. The teams are given a historical SCADA dataset along with information  
229 related with the leakages detected and fixed by the utility throughout 2018, to use for training  
230 purposes and for calibrating their models. It is possible that more leakage events occurred during  
231 2018, however the utility was not able to detect and localize them.

232 Throughout 2019, the utility conducted periodic surveys using additional sensing equipment,  
233 pipe inspections and other methods, and was able to detect and isolate all the leakage events that  
234 occurred within that period. The most critical of these events were repaired, however it was not  
235 possible to repair some of these leakages due to financial reasons.

236 The overall goal of this competition, is to identify methods which are able to detect and localize  
237 the leakage events that occurred in L-Town in 2019, as fast as possible (with respect to time) and as  
238 accurately as possible (with respect to their location), in order to minimize their overall financial

239 costs, both in water losses, as well as due to the hours spent in isolating the leakage by the utility  
240 staff. The L-Town utility will compare the different solutions and select the best one based on that  
241 objective.”

## 242 **SCENARIO GENERATION AND AVAILABLE DATA**

243 To replicate the conditions of a real system, a SCADA dataset was synthetically generated using  
244 simulation, to correspond to sensor measurements from two (2) years of system “operation”. For  
245 the generation of this SCADA dataset, a virtual testbed engine was designed in Python, released  
246 under the EUPL Open Source license (see Data Availability Section). This testbed uses the L-Town  
247 EPANET benchmark, and incorporates a number of assumptions with respect to the hydraulic  
248 solving, the leakage modelling, the modelling of uncertainty as well as the modelling of sensors.

### 249 **Simulation and dataset generation engine**

250 The dataset generation engine takes as input a structured file “dataset\_configuration.yaml”,  
251 which includes the start and end-time of the simulation, the leakages (including the start and end-  
252 time, the leak diameter, the type of the leakage and its peak time), the locations of the sensors (flow,  
253 pressure, AMRs and level sensors).

254 The hydraulic simulations are executed using the Water Network Tool for Resilience (WNTR), a  
255 Python package which supports pressure-driven demand simulations and leakage modelling (Klise  
256 et al. 2017). Specifically, for the pressure-driven demands, we compute a new demand for the  $i$ -th  
257 node  $D_i(k)$ , using the function  $f_{PDD}$ , such that  $D_i(k) = f_{PDD}(p_i(k), d_i(k))$ , where  $p_i(k)$  is the  
258 pressure and  $d_i(k)$  is the requested demand at node  $i$ : If the computed pressure is  $p_i(k) < P_0$  then  
259 the demand is zero, i.e.,  $D_i(k) = 0$ . If the pressure is  $p_i(k) > P_f$ , then the demand equals the  
260 requested demand, i.e.,  $D_i(k) = d_i(k)$ . Finally, in the case where the pressure is  $P_0 \leq p_i(k) \leq P_f$ ,  
261 then the demand is calculated as  $D_i(k) = d_i(k)((p_i(k) - P_0)/(P_f - P_0))^\delta$ . In BattLeDIM, we  
262 consider the following parameters:  $P_0 = 7$ ,  $P_f = 25$ ,  $\delta = 0.5$ . The values for  $P_f$  and  $\delta$  are the  
263 default values used in WNTR, while the minimum pressure value  $P_0 = 7$  was raised from 3.5 to 7  
264 meters since this minimum value was never observed in the L-Town network during the considered  
265 scenarios.

266 Using the pressure dependent demand simulation, the node demand  $D_i(k)$  starts to decrease  
267 compared to the requested demand  $d_i(k)$  when the pressure is below  $P_f$  and goes to zero when  
268 pressure is below  $P_0$ .

## 269 **Nominal and Real models**

270 In practice, it is difficult to have an accurate model of the real system. For this reason, a  
271 “nominal” EPANET L-Town model was provided to the BattLeDIM participants, however a “real”  
272 model (which was unknown to the competitors) was used to generate the SCADA dataset. In  
273 general the nominal model approximates the real, with some uncertainties. The nominal model was  
274 generated by randomizing parameters of the real L-Town network, using the EPANET-MATLAB  
275 Toolkit (Eliades et al. 2016), as follows:

- 276 • Base demand of each consumer type at each node are randomized uniformly between  $\pm 10\%$   
277 compared to the ‘real’ value.
- 278 • Demand patterns: Nominal residential and commercial patterns are available, however  
279 industrial patterns are not available. The patterns used in the ‘real’ model are unique for  
280 each node and may differ significantly from the nominal patterns, while they also include a  
281 significant noise component.
- 282 • Pipe parameter uncertainty: All pipe parameters (roughness, length, and diameter) are  
283 randomized uniformly between  $\pm 10\%$  of their ‘real’ value. This randomization aims to  
284 represent the uncertainty on hydraulic resistance, which is a function of all the aforemen-  
285 tioned pipe parameters. We note that, in reality, parameter uncertainties may have different  
286 magnitudes. Typically, the most uncertain parameter is pipe roughness, while pipe length  
287 and diameter are less uncertain.
- 288 • Topological uncertainty: Two pipes (“p37” and “p251”) were randomly selected to be  
289 closed in the real network, whereas in the nominal model they appeared to be open. The  
290 term “topological” uncertainty is used here to describe the variability of the topological  
291 graph of the network, due to a pipe valve with unknown status (open/closed). This can

292 also be considered as “operational” uncertainty since, typically, valves change status during  
293 operations, such as repairs, that have taken place in the network.

## 294 **Sensors and Telemetry**

295 We assume that there is one (1) tank water level sensor, a total of three (3) flow sensors, one  
296 at the pump and one at each of the DMA entrances, and 33 pressure sensors, all transmitting their  
297 measurements every 5 minutes to the utility’s *Supervisory Control and Data Acquisition* (SCADA)  
298 System. There are no time delays in the data transmission, and no lost packages. Pressure sensors  
299 give an average value of the last 5 minutes, which mitigates the uncertainty due to pressure transients  
300 in the system. In addition, 82 *Automated Metered Readings* (AMRs) have been installed in “Area  
301 C”, for delivering water consumption data directly to the SCADA system. Each AMR gives the  
302 aggregated consumption of many users in the AMR area.

303 The locations of the pressure sensors is depicted in Fig. 3, and the AMRs in Fig. 4. Sensor  
304 readings do not have errors, nor time-delays. The simulated sensor readings are rounded to 2  
305 decimal points; in practice this reduces the amount of data sent over the telecommunications  
306 network.

## 307 **Leakage modelling**

308 We assume that the only faults affecting the system during the 2-year operation, are background  
309 leakages and pipe bursts. Any pre-existing leakages in the network are assumed to be small relative  
310 to individual node demands and have been incorporated into the pressure-dependent demands of  
311 the network. To model the leakage outflow in the  $i$ -th node, we assume the following general model  
312 (Lambert 2001; Greyvenstein and van Zyl 2007; Cassa et al. 2010):

$$313 \quad l_i(k) = L(k)[p_i(k)]^\zeta, \quad (2)$$

314 where  $L(k) = CA(k)\sqrt{2\rho}^\zeta$ , for which the discharge coefficient for turbulent flow is  $C = 0.75$ ,  
315  $A(k)$  is the area of the leak hole which may change in time, and  $\rho$  is the fluid density (for water  
316 we assume that  $\rho = 1000\text{kg}/\text{m}^3$ ). For simplicity, we assume that the pipes in L-Town are made of

317 steel, with roughness coefficients ranging between 120 and 140 (Hazen-Williams). Therefore, the  
 318 exponent related to the characteristics of the leak, is assumed to be  $\zeta = 0.5$ .

319 A key aspect is the leakage magnitude and the time profile of the leakages. There are three (3)  
 320 types of leaks in the system, categorized depending on their magnitude:

- 321 1. **Background leaks:** These are small leaks with size of 0-5% of the average inflow.
- 322 2. **Medium pipe-bursts:** Pipe breaks with flow size of 5-10% of the average inflow.
- 323 3. **Large pipe-bursts:** Pipe breaks with flow size above 10% of the average inflow.

324 In general, the average system inflow for the benchmark is around  $180 \text{ m}^3/\text{h}$ . The concept of  
 325 background leaks is based on the categorization presented in (Lambert 1994); these are leakages  
 326 that may exist in the system undetected for a long period of time. In the proposed benchmark, the  
 327 smallest background leak was constrained at 2.5% of the average inflow, to enable their detection.  
 328 The distinction between medium and large pipe-bursts is made assuming the latter are made visible  
 329 and fixed more quickly by the water utility.

330 Moreover, the leak hole area  $A(k)$  can be time-varying. In the case of abrupt leakage, the hole  
 331 area is zero before the leakage start-time  $T_0$ , and becomes  $\bar{A}$  after that time:

$$332 \quad A(k) = \begin{cases} 0 & k < T_0 \\ \bar{A} & k \geq T_0 \end{cases} \quad (3)$$

333 In the case of incipient leak, we assume that the leak hole area  $A(k)$  gradually increases after  $T_0$ ,  
 334 until it reaches  $\bar{A}$  at time  $T_p$ :

$$335 \quad A(k) = \begin{cases} 0 & k < T_0 \\ \bar{A} \left( \frac{k-T_0}{T_p-T_0} \right) & T_0 \leq k < T_p \\ \bar{A} & k \geq T_p \end{cases} \quad (4)$$

336 Regarding the leak time profile, the following assumptions were made: i) background leaks can  
 337 exist from the beginning of the dataset and continue until the end, or they can start at any given

338 time; ii) there are no large pipe bursts which have started before the simulation time; iii) background  
339 leaks can evolve into bursts (incipient leaks); e.g., a background leak which may have started as a  
340 small crack on a pipe may evolve into a large burst due to the stress applied on the pipe by pressure  
341 transients.

### 342 **Leakage reporting**

343 In practice, large leakages are easier to identify and fix, as they will be reported at some point  
344 by consumers or the utility staff. For the dataset leakages, we assume that large pipe-bursts are  
345 detected and fixed by the water utility, if they reach a flow magnitude larger than  $\bar{l}_j$  at time  $T_l$ . The  
346 time of detection  $T_d$  is a time instance selected randomly during a maximum period of one (1)  
347 week after  $T_l$ . The repair time  $T_r$  is also defined as a time instance defined randomly, within one (1)  
348 week after  $T_d$ . After the leak is fixed, the area of the leak hole becomes zero, i.e.,  $A(k) = 0, t > T_r$ .  
349 Specifically, large and some medium-size leakages (above  $15 \text{ m}^3/h$ ) are fixed by the water utility  
350 after a reasonable time selected in random, with maximum delay of 2 months.

### 351 **Leakage event simulation**

352 All the leakage characteristics, were selected randomly, with certain constraints and assump-  
353 tions:

- 354 • Based on the size of the network, statistically around 15 leakages (background and burst)  
355 events should appear each year in the network, with maximum 20 events. Eventually, we  
356 assume to have 14 events in the year 2018, and 19 events in the year 2019. Four (4)  
357 background leaks in the year 2018 continued in the year 2019. Only large pipe-bursts are  
358 detected and fixed by the water utility.
- 359 • We assume that at most 2 pipe bursts can coexist in the network during the examined periods.  
360 This is to enforce a wider spreading of the leaks during the year.
- 361 • We assume that a leakage can be detected by an L-Town staff using acoustic loggers, within  
362 300 meters radius of its location. This is used in the evaluation of leakage isolation, and is  
363 based on actual feedback received by water utility operators from the original city considered

364 for the L-Town benchmark.

- 365 • We assume that in case leakages exist with overlapping detecting radius, there is a minimum  
366 2 week different between their start time. This is to ensure separability of the alerts during  
367 the evaluation phase.

368 The final leakage locations for year 2018 and 2019 are found in the Fig. 5 and Fig. 6 respectively.

369 The time profile of the leakages in 2019 is depicted in Fig. 7.

### 370 **The BattLeDIM Datasets**

371 The BattLeDIM datasets are composed of the following files, which are openly accessible via  
372 the Zenodo platform (see “Data Availability Statement” section) under the FAIR principles:

- 373 • **Configuration files:** The dataset configuration file indicates the simulation period as well  
374 as the characteristics of the 33 simulated leakages as part of BattLeDIM. It also specifies  
375 the sensors to be included in the SCADA datasets. (File format: YAML)
- 376 • **SCADA datasets:** These correspond to the SCADA measurements during the 2-year period  
377 between 2018-01-01 00:00 until 2019-12-31 23:55, at 5-minute time steps. The SCADA  
378 datasets are comprised of the water tank level, the flow sensors, the AMR measurements  
379 and the pressure sensors. (File format: CSV)
- 380 • **Leakages:** Table of times with respect to the leakage events of BattLeDIM, indicating their  
381 outflows in  $m^3/h$ . (File format: CSV)
- 382 • **Fixed Leakages reports:** This includes the repair times of pipe bursts that have been fixed  
383 in 2018 by the water utility. (File format: TXT)
- 384 • **Network models:** Two network models are provided. i) The “*real*” model is the one used to  
385 generate the 2-year datasets, along with all the demand patterns. It contains the real network  
386 parameters and consumer demands. It does not contain any leakages. The real network  
387 should be considered as “unknown” ii) The “*nominal*” model should be used as the “known”  
388 model. This network is provided with nominal parameters for all the system elements. The  
389 nominal base demands for each node are based on average historical metered consumption.

390 Weekly demand profiles for three consumer types (residential, commercial and industrial)  
391 are also provided, however they do not capture the yearly seasonality. Furthermore, the  
392 EPANET model parameters may be different from the actual network parameters (e.g.,  
393 diameters, roughness coefficients), and this difference is no greater than 10% of the nominal  
394 values. (File format: INP)

## 395 **LIMITATIONS**

396 The main challenge in developing effective leakage diagnosis algorithms is for them to be  
397 applicable in real systems and be able to deal with the problems arising from the scarcity and  
398 reliability of the data collected from the field. The aim of the proposed benchmark is to offer a  
399 realistic simulation scenario, built upon the expertise of practitioners, which closely resembles real  
400 conditions. It has the advantage that all the parameters and aspects of the system operation are  
401 known, and thus it can be used to compare and evaluate different methodologies. However, it has  
402 limitations and differences from real systems which are stated in this section to advice caution to  
403 researches and practitioners when using the benchmark.

404 The realistic demands included in this benchmark were generated by analyzing demands from  
405 real networks into their components and reproducing them by randomizing the components as  
406 described in (Vrachimis et al. 2018c). Real network demands may vary compared to the proposed  
407 approximations. Moreover, pressure-driven analysis is used to make the demands more realistic;  
408 however, we note that more research may be needed in selecting appropriate values for the pressure-  
409 driven analysis parameters.

410 A realistic leakage modeling approach was followed in this work by modeling pressure-  
411 dependent leakages on pipes, while the leakage function is constructed such as to exhibit time-  
412 variability with respect to the orifice size. However, the function describing leakage flow may vary  
413 in practice, because data collection about the size of leaks found in the field is a challenging task.  
414 More realistic leakage functions, than the one used in equation (2), have been proposed in recent  
415 literature (van Zyl et al. 2017; Kabaasha et al. 2020) and may be considered in future versions of  
416 this benchmark.



417 A decision was made in the creation of this benchmark to not include sensor time-delays  
418 and errors. This was taken consciously to avoid an extra dimension of complexity to a difficult  
419 competition problem, which includes large model uncertainties and small number of sensors  
420 compared to the system size. Moreover, we wanted the participants to focus on leakage diagnosis  
421 methodologies and not on methodologies for data validation. However, data acquired from real  
422 sensors may include significant errors and a number of measurements may need to be discarded  
423 and reconstructed. The real-time processing of data may be impeded by measurements arriving at  
424 later time-steps or never arriving at all.

425 This benchmark does not take into account events that may happen during and after repair  
426 works. Typically, repairs require the isolation of network sections by closing valves, an action that  
427 may cause pressure increase in the network. A typically observed phenomenon is the increase of  
428 leakage flows in other parts of the network during repairs or, in the worst cases, new pipe bursts. The  
429 risk of causing new leakages during repairs was not taken into account and should be considered  
430 when using this benchmark to test leakage diagnosis methodologies designed for application on  
431 real systems.

432 The reward for detecting leakages is based only on the value of water lost. However, the reward  
433 could be higher if indirect costs due to water losses were taken into account. The indirect costs  
434 include the acceleration of pipe deterioration, as well as third party damages. Such effects are  
435 usually accounted for in the cost of water, however they are difficult to quantify and were not  
436 considered in the benchmark.

## 437 **COMPETING LEAKAGE DETECTION AND ISOLATION METHODS**

438 In the following paragraphs we provide a short overview of the methodologies proposed by the  
439 competing teams.

440 The *Cheng00* team ([Cheng et al. 2020](#)) resorted to a three-stage approach involving simulation,  
441 ensemble multivariate change point detection (EMCPD), and statistical analysis. Pressure and flow  
442 residual time series are first obtained by comparing the SCADA datasets with those of simulated  
443 normal operation, produced with the provided benchmark model. The residuals are then analyzed

444 with EMCPD to obtain a rough estimate of the occurrence of leak events in space and time. The  
445 final localization is performed after interpolating nodal pressures around likely candidate positions  
446 and by isolating the most likely sites with a two-sample one-sided Student's t-test.

447 The *DandW* team (Huang et al. 2020; Huang et al. 2022) proposed a methodology that treats  
448 each area of the L-Town network in Fig. 1 separately. This methods exploits the provided benchmark  
449 model to estimate expected sensor readings during normal operations and compute the residuals  
450 with respect to the provided SCADA data. Sensitivity vectors are then computed for each pipe as  
451 the Jacobian matrix of nodal pressures to pipe flows. The *angle method*, which involves calculating  
452 the angle between the residual vectors and the sensitivity vectors, is then used to isolate leaky pipes.  
453 These are characterized by having the smallest angles.

454 The *Leakbusters* team (Daniel et al. 2020; Daniel et al. 2022) tackled the challenge with a  
455 high-resolution pressure-driven method for leakage identification and localization composed of  
456 two sequential modules. In the first module, linear regression models are calibrated using data  
457 with no leaks to predict pairwise sensor pressure readings. When fed with new SCADA data, the  
458 reconstruction error between predicted and observed readings is tracked to identify the start time  
459 of a potential leak and the location of its nearest sensor. The second module uses the start time and  
460 most affected sensors reported by the first module to pinpoint leaky pipes relying on an initial set  
461 of candidate pipes and the application of a simulation-based optimization framework with iterative  
462 linear and mixed-integer linear programming.

463 The *CIACUA* team (Saldarriaga et al. 2020) approached the BattLeDIM problem by resorting  
464 to anomaly detection analysis and a simulation-optimization framework involving EPANET and  
465 Genetic Algorithms (GA). Anomaly detection analysis was first carried out by comparing SCADA  
466 data and the output of EPANET models. If the error between any observed and predicted signals  
467 passed a certain threshold, simulation-based optimization with GA was used to find which location  
468 would best explain such discrepancy, thus identifying the leaking pipe. Emitter equations were  
469 used to simulate leaks in the EPANET model.

470 The *Tsinghua* team (Wang et al. 2020; Wang et al. 2022) employed a hybrid approach where

471 statistical methods are used in combination with hydraulic modelling. Their scheme comprises  
472 three stages. In the estimation stage Empirical Model Decomposition (EMD) and Vector Auto  
473 Regressive models are used to estimate expected flow and pressure in normal conditions. The  
474 residuals between these expected values and observed SCADA data are further processed in the  
475 identification stage to place leaks in time, and infer their size. In the final localization stage, leaking  
476 pipes are isolated by a double comparison between observed and simulated (EPANET) pressure  
477 data for the week with the suspected leak and the one preceding it.

478 The *Under Pressure* team (Steffelbauer et al. 2020; Steffelbauer et al. 2022) also employed a  
479 hierarchical approach made of 3 stages. Similar to the *Tsinghua* team, in the first stage demand  
480 calibration for the entire network was inferred from AMR data on Zone C using EMD. The authors  
481 also performed a calibration of the roughness coefficient using weighted least squares problem with  
482 bounded constraints. The second stage of *Under Pressure*'s approach entails the creation of a *dual*  
483 hydraulic model for leak detection. In this dual model, the pressure drops due to a leak translate  
484 into additional outflows to virtual reservoirs connected to the pressure measurement nodes. These  
485 time series, and the derived residuals, have a much better signal-to-noise ratio which facilitates  
486 detection and localization. This is done in the third stage, where leaks are first identified in time  
487 with the help of change detection methods (CUSUM, likelihood-ratio) and GA. The leaking pipe  
488 is then isolated based on the computation of Pearson correlation between residuals of virtual leak  
489 flows and pipe sensitivities, similar to what done by the *DandW* team.

490 *Fuzzy* methods are at the core of the *Zhiyun Shuiwu* team (Zhang et al. 2020). In the first  
491 stage, Deep Fuzzy Mapping is used to calibrate model demands from observations. Secondly, leaks  
492 are identified in time based on anomalies between observed and modeled pressure values and an  
493 analysis of the most affected nodes. Localization is finally performed based on fuzzy similarity  
494 between real bursts characteristics and pipe network characteristics.

495 The *IRI* team (Romero et al. 2020; Romero-Ben et al. 2022) devised a data-driven approach for  
496 Area A of L-Town due to the high density of pressure sensors. On the other hand, a model-based  
497 approach is used for both Area B and Area C to respectively overcome the lack of pressure sensors

498 and exploit the availability of AMRs. In the data-driven approach, graph-based interpolation is first  
499 performed to estimate the state of the entire network from available data of leaky and non-leaky  
500 scenarios. The selection of candidate leak location is then performed by nodal pressure comparison  
501 between these estimated states. In the model-based approach, EPANET simulations are carried out  
502 after inferring the demands for Area B and Area C. The results of the simulations with leaks added  
503 at different locations are compared against the SCADA data to find the most likely placement for  
504 the leak.

505 The *KU Hydrosystems* team (Min et al. 2020) proposed a two-stage method where leak iden-  
506 tification in time and space is tackled separately using a data-driven and a model-based approach.  
507 After pre-processing the data and performing feature selection, the detection of the leak in time  
508 is performed jointly by resorting to k-means clustering. Leak locations are then identified via a  
509 comparison between real data and the output of multiple simulations using a calibrated EPANET  
510 model accounting for leaks (with emitter coefficients). The initial calibration is performed with  
511 the Harmony Search algorithm in order to find optimal values of roughness coefficients and nodal  
512 demands.

513 *InfraSense Labs* (Blocher et al. 2020) devised a method involving three main steps. Firstly,  
514 the daily demand profiles are partitioned into clusters using the k-means algorithm. The clusters  
515 correspond to days with similar flow patterns so that variations in the derived clusters can be used to  
516 identify changes in demand that may be attributed to leaks. Leaks are then detected by comparing  
517 the difference between expected demands (derived from flow profiles of five preceding days based  
518 on cluster membership) and observed flows. If the residuals indicate the presence of a leak, hot-  
519 spots are localized by solving a regularized inverse problem that includes a pressure-driven model  
520 for the leak flow.

521 *DHI China* (Liu et al. 2020) proposed a method that relies on genetic algorithms and Machine  
522 Learning (ML) techniques. GA is used to calibrate the provided nominal model, whose demand  
523 patterns are defined based on the analysis of the provided AMR data. Leak detection in time is  
524 done with the use of both Deep Learning methods (an LSTM neural network) and gradient boosted

525 trees (LightGBM). GA-based simulation-optimization (with EPANET) is employed to localize the  
526 leaky pipe, similar to what done by other teams.

527 The Multiple Leaks Detection and Isolation Framework (MLDIF) proposed by the *Tongji* team  
528 (Li and Xin 2020) consists of three stages as “calibration-identification-localization”. First, a  
529 model calibration stage is performed to get a calibrated hydraulic model using a time-period where  
530 little or no leakages are assumed to exist. Any pre-existing leakages in the selected time-period are  
531 incorporated into the calibrated model, which is then used to estimate the overall yearly leakage flows  
532 and to predict nodal pressures under a ‘leak-free’ scenario. Then, the pressure residuals between  
533 observed and predicted pressure are processed by integrating STL decomposition method and the  
534 K-means clustering method to identify different leak scenarios during the analysis period. Finally,  
535 by adding no-repaired but identified leaks to the calibrated hydraulic model in the localization stage,  
536 a new and simple leakage scenario is reconstructed to facilitate leakage localization. Therefore,  
537 the pipe with the highest probability of leakage can be isolated by a step-wise method based on  
538 matching degrees between the actual leakage feature and the simulated leakage features.

539 The *Wu BSY* team (Wu and He 2020) presented an integrated data analysis with hydraulics-  
540 based modeling approach consisting of three main steps: i) *data pre-processing* to prepare for  
541 analysis, where flow and pressure time-series are decomposed to get rid of trend and seasonality  
542 using the Seasonal-Trend decomposition procedure ; ii) *data analysis* for leakage event detection,  
543 where the decomposed time-series are analyzed using Statistical Process Control methods; and iii)  
544 *model analysis*, where simulation-based optimization in *Bentley WaterGEMS*, a hydraulic model  
545 calibration tool, is used to localize the leaky pipes using a pressure-driven approach where the  
546 emitter coefficients and locations are the parameters to be optimized.

547 The *CUBALYTICS* team (Bhowmick and Seifert 2020) also devised an approach combining  
548 data-driven methods with hydraulic simulations. This method is based on the computation of an  
549 *anomaly matrix* (AM) for leak detection and localization. This matrix is created by first applying  
550 statistical methods to identify anomalies in the Master Data Set, i.e., the overall table having  
551 timestamps as indexes and sensor readings as columns. The AM is a binary matrix (1 = anomaly

552 detected), obtained from the previous operation after keeping only the rows for which there is at  
553 least an anomaly. Leaks are identified in time by analyzing contiguous rows in the AM having  
554 multiple anomalies. The list of nodes, i.e., the headers of all columns with non-zero entries, is  
555 checked to find valid node combinations identifying potential leaky pipes. The isolated pipe for  
556 each leak is selected after comparison with pressure-driven simulations.

557 Decision trees are at the core of the methodology of the *Artesia* team ([Adanza Dopazo 2020](#)).  
558 The approach consists of three main steps. In the first step, data normalization and feature  
559 engineering is performed to extract minimum and maximum daily peaks, as well as averages for  
560 different parts of the day for all pressure, water level and flow sensors. Decision trees are then  
561 trained on this refined dataset to predict the mean night pressure values expected for each pressure  
562 sensor. The mean pressure during the night is chosen as the target to predict since pressure during  
563 this time of the day is more steady and less affected by randomness. In the last stage, the differences  
564 between predicted and observed mean night pressure values in the test dataset are used to identify  
565 leaks in time, while comparison of results across neighboring pressure sensors is used to improve  
566 localization.

567 The *DHI Singapore* team ([Tan et al. 2020](#)) employed WNTR, a Python wrapper of EPANET, to  
568 generate extra data for training a deep neural network (DNN) using Tensorflow. Before generating  
569 the leak events, the team calibrated the provided nominal model to find optimal values of pipe  
570 diameters, roughness coefficient, as well as determining optimal seasonality of residential and  
571 commercial demands. Calibration was performed using GA and the 2018 pressure readings.  
572 The DNN development dataset is generated from 400 simulations with random leaks at different  
573 locations, with different start time and duration. A five hidden layer DNN is trained on this data  
574 to isolate the leaky location having as inputs the readings from the 33 pressure sensors. After its  
575 validation, the DNN is tested on the competition dataset.

576 The *UNIFE* team ([Marzola et al. 2020](#); [Marzola et al. 2022](#)) adopted a pragmatic approach  
577 to detect and localize leakage events, based on the analysis of the SCADA data and the use of  
578 the provided hydraulic model of the network. After inferring demand patterns for the entire

579 network based on the provided AMR data, the hydraulic model is calibrated (roughness and  
580 diameters) to realistically represent the hydraulic behaviour of the network. The observed inflows  
581 and water demands are then analysed to identify leakage number, entity and time of occurrence with  
582 engineering judgment. Each identified leakage is then spatially localised through an enumerative  
583 procedure. This is done by i) performing simulation after assigning the leakage to each pipe of  
584 the network in turn, ii) assessing the error in terms of differences between observed and simulated  
585 pressures, and iii) selecting the pipe characterized by the lowest error.

586 The *FluIng* team (Barros et al. 2020) resorted to a mixed approach using signal processing for  
587 leak identification, and simulation-based optimization for leak localization. The first phase of leak  
588 identification entails the use of blind source separation to decompose each measured flow time  
589 series into a main signal, primarily related to water consumption, and a "noisy" signal in which  
590 leak events are more visible. Change detection is then performed on this noisy component to detect  
591 leaks in time. Localization of leaky pipes is then carried out with a two-steps approach based on  
592 Particle Swarm Optimization where i) the provided nominal model is first calibrated in an *offline*  
593 fashion, and ii) leak locations are inferred via iterative *online* fine tuning of nodal demands.

## 594 **Analysis of methodologies**

595 Table 1 summarizes the key elements of each method, highlighting similarities and differences  
596 between them. The general features which are listed in Table 1 and their use as part of the different  
597 methodological approaches is described in Table 2.

598 In general, the solutions proposed may be comprised of one or more of the following parts:  
599 the detection procedure, the localization approach, and the calibration method. Each methodology  
600 utilized various tools in order to solve each problem. For example, some model-based approaches  
601 relied on the use of nominal water network models provided (such as the EPANET L-Town model).  
602 To accommodate the differences between the measurements and the nominal model, calibration  
603 methods were used to design a more accurate representation, by updating the demands and certain  
604 pipe parameters. The calibrated model can be used to create datasets describing the operation of  
605 the system under normal and faulty operation conditions, e.g., using the EPANET libraries. This

606 can allow the comparison of the computed pressure residuals with the observed pressure sensor  
607 measurements.

608 Another approach is to consider the mathematical model of the system, to create a *pressure*  
609 *sensitivity matrix*, through a linearization of the hydraulic equations. Using the above, residuals  
610 can be computed, using model-based approaches which compare simulation-based estimations and  
611 SCADA measurements, as well as by using model-free approaches. The residuals, as well as other  
612 relevant time-series, can be analyzed using change detection techniques (CUSUM, angle method  
613 etc.), time series analysis and signal processing, empirical method decomposition, regression  
614 analysis, hypothesis testing and other statistical approaches. More advanced statistical approaches,  
615 such as machine learning, and computational intelligence methods based on fuzzy systems, have  
616 also been proposed.

617 A subset of methodologies considers optimization formulations, which may rely on simula-  
618 tions to evaluate the objective functions, or on explicit mathematical formulations which can be  
619 solved using Integer/Dynamic/Mixed Integer Programming. Where this is not possible due to the  
620 complexity of the optimization formulation, meta-heuristics (such as genetic algorithms or particle  
621 swarm optimization) can be used. Finally, it's important to note that some approaches analyzed the  
622 AMR-area in a different way, by creating a model of the water demands in the area, to exploit the  
623 additional information provided due to the significant penetration of the smart meters.

## 624 **EVALUATION PROCEDURE**

625 Participants were required to submit their results in the format specified in a template file,  
626 which includes the location and start time of each detected leakage event. The start time of a  
627 leakage is specified in the ISO 8601 time format YYYY-MM-DD hh:mm. The location of the  
628 leakage is specified by the link ID, as defined in the EPANET model of the network "L-Town.inp".  
629 Participants were allowed to specify any number of leaks.

## 630 **Competition evaluation criteria**

631 Evaluation of participant results follows a pure economic approach. The water utility of L-Town  
632 calculates the profit from water saved in a single year from successful detections. The utility also



633 considers the cost of the repair crew every time it is sent to search for a leakage.

634 A correct detection is one that points at a link ID which is inside a predefined pipe length  
635 radius around the leak location, and the given leakage start time is during the lifetime of the same  
636 leakage. The predefined pipe radius is defined by the capability of the close range equipment used  
637 by the repair crew (e.g. acoustic sensors) to exactly pinpoint the location of the leakage in a single  
638 workday.

639 The scoring methodology is described here in detail. Given a user defined set of detections  
640  $\mathcal{D}$  and the set of leakages  $\mathcal{L}$  (2019 BattLeDIM dataset), the total score  $S$  is calculated using the  
641 following rules:

1. **True detection (True Positive):** A given detection  $i \in \mathcal{D}$  is considered a True Detection of a leakage  $j \in \mathcal{L}$  if the detection time  $t_d^i$  and the distance  $x_{ij} \geq 0$  from the center of the isolated link to the leak location, satisfy the following conditions:

$$t_{st}^j \leq t_d^i \leq t_{end}^j, \quad (5a)$$

$$x_{ij} \leq x_{max}, \quad (5b)$$

642 where  $t_{st}^j$  and  $t_{end}^j$  are the start and end time of leakage  $j$  respectively, and  $x_{max}$  is the  
643 predefined pipe length radius around the leak location.

2. **False detection (False Positive):** False detections are the detections which do not satisfy the True detection condition above.
3. **Missed detection (False Negative):** Missed detections are the set of leakages in  $\mathcal{L}$  which have not been detected by any detection in  $\mathcal{D}$  (includes 4 leakages starting in 2018 and 19 leakages starting in 2019).
4. **Order of evaluation:** Detections in  $\mathcal{D}$  are evaluated in chronological order, i.e., from the earliest detection to the latest detection, against all leakages in  $\mathcal{L}$ . Note that detections given by participants which are outside the year 2019 are ignored.
5. **Repeated detections:** Once a leak is detected, it is added to the list  $\mathcal{L}_\uparrow$ . Successful

653 detections of leaks in  $\mathcal{L}_\Gamma$  are given a score of zero (0), i.e., repeated detections of the same  
 654 leakage are ignored.

655 **6. Multiple detections:** A single detection may detect only one leakage, even if more than  
 656 one leakage is in the detection area. Note that detection of multiple leakages is limited due  
 657 to the leakage placement algorithm used to create the dataset. In the case of the existence  
 658 of multiple leakages in the detection radius of detection  $i$ , e.g., leakage  $j \in \{1, \dots, m\}$ ,  
 659 only the leakage closest to the detected link is considered to be discovered. The discovered  
 660 leakage  $l \in \mathcal{L}$  in the case of multiple true detections is given by:

$$661 \quad l = \{j : x_{ij} = \min(x_{ij}, j \in \{1, \dots, m\})\} \quad (6)$$

662 **7. Profit from water saved:** The profit  $p_w^i$  (euro) from water saved by detection  $i$ , for a  
 663 detected leakage  $j$ , is calculated as follows:

$$664 \quad p_w^i = \left( \sum_{k=t_d^i}^{t_{end}^i} q^j(k) \Delta t \right) c_w, \quad (7)$$

665 where by detection  $i$ ,  $q^j(k)$  is the flow rate of leakage  $j$  at each discrete time step  $k$ ,  $\Delta t$  is  
 666 the duration of the discrete time step and  $c_w$  is the cost (euro) of water per cubic meter.

667 **8. Repair crew cost:** All detections in  $\mathcal{D}$  are associated with a utility repair crew cost. The  
 668 repair crew checks for leakages only within a predefined radius of  $x_{max}$  from the given  
 669 location. The repair crew cost for a given detection  $i$  is assumed to be proportional to the  
 670 distance  $x_{ij}$  from the leakage  $j$  and is calculated as follows:

$$671 \quad c_r^i = \begin{cases} -\left(\frac{x_{ij}}{x_{max}}\right) c_r, & x_{ij} < x_{max} \\ -c_r, & x_{ij} \geq x_{max} \end{cases} \quad (8)$$

672 where  $c_r^i$  is the repair crew cost for detection  $i$ , and  $c_r$  is the maximum repair crew cost for  
 673 a given leakage search assignment.

674 **9. Total score:** The total score  $S$  for a given set of detections  $\mathcal{D}$  is given by:

$$675 \quad S = \sum_{i \in \mathcal{D}} s^i = \sum_{i \in \mathcal{D}} (p_w^i + c_r^i), \quad (9)$$

676 where  $s^i$  is the score per given detection  $i$ .

677 The parameters of maximum detection radius  $x_{max}$ , cost of water per cubic meter in euro  $c_w$   
678 and the maximum repair crew cost  $c_r$  are given in Table 3. The cost of water is selected assuming  
679 a water utility which operates in Cyprus. The maximum repair crew cost is calculated assuming  
680 a three-person repair crew searching for the leakage location for a whole 8-hour workday, with an  
681 hourly rate of approximately 20 euro per hour. The maximum detection radius is selected assuming  
682 the repair crew is able to search using acoustic sensors a maximum pipe length of 1 km in a single  
683 workday. In order for this distance to be translated into a radius, an average of three pipe branches  
684 emerging around any given location is assumed. The maximum score in this problem, given the  
685 parameters of Table 3 and the leakages existing in the dataset, is achieved when all leakages are  
686 detected at their exact start time and location, while no false detections are given. The “perfect”  
687 score of the competition was calculated using equation (9) to be €523,124.

688 For illustration purposes, an example of the evaluation function is shown in Fig. 8, where  
689 all possible values of the detection score are plotted for detecting a leakage with constant flow of  
690  $q(k) = 100 \text{ m}^3/h$ . The evaluation parameters were arbitrarily chosen as follows: cost of water  
691  $c_w = 1 \text{ euro/m}^3$ , max crew cost  $c_r = 500 \text{ euro/detection}$  and max detection distance  $x_{max} = 50m$ .

### 692 **Alternative evaluation criteria**

693 The evaluation methodology used in this competition has some disadvantages which arise from  
694 using a score which is proportional to the amount of water saved from each successfully detected  
695 leakage. Specifically, the current methodology favors the detection of large and abrupt leakages as  
696 well as leakages which start early in the dataset.

697 To avoid this issue, an alternative evaluation approach is demonstrated which takes into account  
698 the total volume of water lost from each leakage, given in Fig. 9. The volumes are derived by

699 calculating the area under the leakage flow curves of Fig. 7. It can be observed from Fig. 9 that  
700 each leakage will be rewarded differently since the reward for each detection directly relates to the  
701 water volume loss of each leakage.

702 This alternative evaluation approach alters the reward function of (7) which calculates the profit  
703 from each detected leakage, by normalizing the profit by the volume of the corresponding leakage.  
704 Specifically, given detection  $i$  which successfully detects leakage  $j$ , the profit from water saved  
705 (euro) is calculated as follows:

$$706 \quad p_w^i = \frac{v_s^j}{v^j} v_m c_w \quad (10)$$

707 where  $v_s^j$  is the volume of water saved given detection  $i$ ,  $v^j$  is the total volume of water loss from  
708 leakage  $j$ , and  $v_m$  is the mean volume of water loss of all leakages in the dataset. The mean leakage  
709 volume  $v_m$  is calculated for this dataset to be  $v_m = 28432 \text{ m}^3$ .

710 Notice that using the normalized reward function, the maximum reward for each detected  
711 leakage is  $v_m c_w$ . The most obvious drawback of this alternative evaluation approach is that the  
712 Economic score loses its literal meaning.

## 713 **COMPETITION RESULTS AND DISCUSSION**

714 Team rankings are defined by calculating the *Economic* score of the results submitted by each  
715 team. The Economic score of each team is given in Fig. 10(a), where the names of the teams  
716 have been substituted by generic labels, specifically the letters A–R. It is interesting to note that  
717 the Economic score does not necessarily reflect the ranking when the True Positive Rate (TPR)  
718 and False Positives (FP) of each submitted result is considered. The TPR and FP of each team are  
719 illustrated in Fig. 10(b) and Fig. 10(c) respectively.

720 The winning teams of the BattLeDIM competition, were the 6 teams with the highest economic  
721 score and with the highest true-positive rate. The name of these teams are provided in Table  
722 4, along with their Pareto ranking. For instance, “Tongji-Team” and “Under Pressure” are non-  
723 dominated solutions and are ranked to the first Pareto front with an economic score of €264,873  
724 and €260,562, and a True Positive Rate of 56.52% and 65.22%, respectively. The “Perfect” score

725 of the competition was €523,124 (no time delay in detection, no false positives, exact position),  
726 which implies that the best solutions in BattLeDIM achieved a score around 50%.

### 727 **Evaluation parameter sensitivity analysis and alternative criteria results**

728 The sensitivity of the total score to the cost of water per cubic meter in euro  $c_w$  is evaluated  
729 here in order to analyze the effect that different assumptions on cost may have on the ranking of  
730 solutions provided. The cost of water affects the Economic score the most since this is proportional  
731 to the amount of water lost from leakages, while it does not affect the number of True Positives  
732 or False Positives achieved by each team. Five different water prices were used to re-evaluate the  
733 competition results ranging from  $0.40 \text{ €/m}^3$  to  $1.20 \text{ €/m}^3$ .

734 The sensitivity analysis results are illustrated in Fig. 12. The results indicate that the increasing  
735 water price favors teams which had a larger number of False Positives and of which the Economic  
736 score was affected due to the cost of sending out repair crews. This result draws the conclusion that,  
737 given a difficult challenge such as the BattLeDIM problem, the cost of water should be taken into  
738 account when deciding how conservative a leakage diagnosis methodology should be. Another  
739 interesting observation is that the first five teams do not change rank with the increasing water price  
740 since they outperform the rest of the methodologies in the TPR metric.

741 Moreover, the results using the alternative evaluation criteria described in Section 7 are shown  
742 in Fig. 13. It can be observed that the normalized score rankings follow more closely the rankings  
743 of the True Positive Rates, except in the cases where the corresponding teams have a high number  
744 of False Positive detections.

### 745 **Discussion**

746 The BattLeDIM competition provides valuable insights on the state-of-the-art in leakage de-  
747 tection and isolation methods, their limitations as well the different ways that the results should be  
748 evaluated. For instance, by analyzing the methodological approaches followed by the top teams,  
749 as shown in Table 1, it is apparent that different approaches have been used by the teams, and the  
750 robustness of each approach to different evaluation functions may vary. Some of the observations  
751 are discussed below:

- 752
- Most top-scoring teams make use of a nominal model, of which the parameters are calibrated  
753 in some form using sensor data, to construct a water distribution model which describes  
754 the normal operation of the system (such as Tsinghua, Under Pressure, IRI and UNIFE),  
755 by incorporating existing leakages into the calibrated node demands. This allows the  
756 computation of the expected flows and pressures at different locations in the network.  
757 Moreover, they also consider the AMR measurements separately from the rest of the network,  
758 and use them to estimate/calibrate demands.
  - For the detection of events, model-based residuals along with some form of a change  
759 detection algorithm (e.g., Leak-Busters, UNIFE, Under Pressure) or time-series/signal pro-  
760 cessing (e.g., Tongji) analysis was preferred by most of the top-scoring teams. Some of  
761 these residuals were also utilized for localization purposes (e.g., IRI, Tsinghua).
  - For the leak isolation, top-scoring teams used some form of optimization framework, to  
762 identify the most likely leakage point (e.g., Leak-Busters, Tsinghua, IRI and Tongji).
  - Some solutions, had a high True Positive Rate, but with a significantly higher number of  
763 False Positives (210) with respect to the other participants (such as team ‘E’ in Fig. 10).  
764 Based on the BattLeDIM assumptions for the cost of water and staff cost, this solution  
765 received a low score. However, sensitivity analysis of the result indicates that, for higher  
766 cost of water, this solution could have received a higher rank. This indicates that it may be  
767 beneficial to accept higher number of false positives, if the cost of water lost is significantly  
768 higher than the staff cost.  
769  
770  
771

## 772 **CONCLUSIONS AND OPEN CHALLENGES**

773 In this paper we presented the results from the “Battle of the Leakage Detection and Isola-  
774 tion Methods” (BattLeDIM), an open competition which aimed to objectively compare different  
775 methodologies in their ability of detecting and isolating leakage events within a virtual water  
776 distribution system. For the purposes of this work, a new benchmark network was introduced,  
777 “L-Town”, based on a realistic water distribution system. Moreover, a synthetic 2-year SCADA  
778 benchmark dataset was generated with leakages of various types and magnitudes, which can be

779 used by the research community to develop leakage diagnosis methodologies, keeping in mind the  
780 limitations of this benchmark mentioned in Section 5. An economic objective metric was defined  
781 to evaluate the different solutions, considering realistic operational costs. In total, 18 teams from  
782 the academia and the industry participated in the BattLeDIM competition. The teams used various  
783 methodologies, including model-based and model-free approaches, simulation and optimization  
784 tools, machine learning and others; these techniques are summarized in Table 2. We presented the  
785 evaluation methodology and discussed its limitations.

786 Overall, the competition demonstrated that multiple technologies could be used for solving the  
787 problem and that there is potential for significant improvement, since the top solutions achieved  
788 50% of the maximum possible score. However, it is important to make a distinction between the  
789 ‘maximum possible score’ and the ‘maximum feasible score’ in this problem: the former is the  
790 score achieved when all leakages are detected perfectly without false positives, while the latter  
791 is the maximum score that can be achieved by any methodology given the limited information  
792 provided about the problem. The methodology to calculate the maximum feasible score for the  
793 BattLeDIM benchmark is an open research question. Since the goal of this benchmark is to recreate,  
794 as realistically as possible, a real-world problem, the development of such methodology will be  
795 useful in determining the conditions that should exist in real systems to make it at least theoretically  
796 feasible to achieve a certain performance in leakage diagnosis. Many factors are in play that affect  
797 the maximum feasible score, such as the selected water network, the size of leakages and the  
798 magnitude of the considered uncertainty. Moreover, it is safe to say that the maximum feasible  
799 score will change by varying some parameters of the BattLeDIM problem to make it even more  
800 realistic; for example, including sensor noise and missing measurements in the dataset.

801 In closing, the BattLeDIM competition demonstrated the need for open benchmarks, which can  
802 assist the research community towards reproducibility and open science.

## 803 **DATA AVAILABILITY STATEMENT**

804 All data, models, or code generated or used during the study are available in a repository online  
805 in accordance with the FAIR data retention policies, under the European Union Public License

806 (EUPL) v1.2:

- 807 • Dataset generation and scoring algorithm: <https://github.com/KIOS-Research/BattLeDIM>
- 808 • SCADA Dataset: <https://zenodo.org/record/4017659>
- 809 • Reproducible code: <https://codeocean.com/capsule/2366240/tree/v1>

## 810 **ACKNOWLEDGMENTS**

811 This work was supported by the European Research Council (ERC) under the ERC Synergy  
812 Grant ‘Water-Futures’ (Grant agreement No. 951424); by the European Union Horizon 2020  
813 programme Grant Agreement No. 739551 (KIOS CoE), and the Government of the Republic of  
814 Cyprus through the Deputy Ministry of Research, Innovation and Digital Policy; by the Interreg V-  
815 A Greece-Cyprus 2014-2020 program, co-financed by the European Union (ERDF) and National  
816 Funds of Greece and Cyprus under project “SmartWater2020”; by the WaterAnalytics Project  
817 ENTERPRISES/0916/23 which is co-financed by the European Regional Development Fund and  
818 the Republic of Cyprus through the Research and Innovation Foundation; and by the Deutsche  
819 Forschungsgemeinschaft (DFG).

## 820 **REFERENCES**

- 821 Adanza Dopazo, D. (2020). “A leakage detection system extracting the most meaningful features  
822 with decision trees..” *Zenodo*, <10.5281/zenodo.3906668> (June).
- 823 Barros, D., Resende, P., Brentan, B., Meirelles, G., Montalvo, I., Luvizotto, E., and Izquierdo,  
824 J. (2020). “Signal processing and optimization process for leakage detection and localization.”  
825 *Zenodo*, <10.5281/zenodo.4011894> (September).
- 826 Bhowmick, S. and Seifert, K. (2020). “Water Leakage Detection and Localization: Anomaly Matrix  
827 - A Deterministic Approach.” *Zenodo*, <10.5281/zenodo.3906850> (June).
- 828 Blocher, C., Pecci, F., Jara Arriagada, C., and Stoianov, I. (2020). “Detecting and localizing  
829 leakage hotspots in water distribution networks via regularization of an inverse problem: An  
830 application to the battle of leakage detection and isolation methods 2020 competition.” *Zenodo*,  
831 <10.5281/zenodo.3921800> (June).



832 Casillas, M., Puig, V., Garza-castañón, L., and Rosich, A. (2013). “Optimal sensor placement  
833 for leak location in water distribution networks using genetic algorithms.” *Sensors*, 13(11),  
834 14984–15005.

835 Cassa, A. M., van Zyl, J. E., and Laubscher, R. F. (2010). “A numerical investigation into the effect  
836 of pressure on holes and cracks in water supply pipes.” *Urban Water Journal*, 7(2), 109–120.

837 Chan, T. K., Chin, C. S., and Zhong, X. (2018). “Review of current technologies and proposed  
838 intelligent methodologies for water distributed network leakage detection.” *IEEE Access*, 6,  
839 78846–78867.

840 Cheng, T., Li, Y., Harrou, F., Sun, Y., Gao, J., and Leiknes, T. (2020). “A hybrid leakage detection  
841 and isolation approach based on ensemble multivariate changepoint detection methods.” *Zenodo*,  
842 <10.5281/zenodo.3964167> (June).

843 Cuguero-Escofet, M. A., Puig, V., and Quevedo, J. (2017). “Optimal pressure sensor placement  
844 and assessment for leak location using a relaxed isolation index: Application to the Barcelona  
845 water network.” *Control Engineering Practice*, 63, 1–12.

846 Daniel, I., Pesantez, J., Letzgus, S., Khaksar Fasaee, M. A., Alghamdi, F., Berglund, E.,  
847 Mahinthakumar, G., and Cominola, A. (2022). “A Sequential Pressure-Based Algorithm for  
848 Data-Driven Leakage Identification and Model-Based Localization in Water Distribution Net-  
849 works.” *Journal of Water Resources Planning and Management*, 148(6), 04022025.

850 Daniel, I., Pesantez, J., Letzgus, S., Khaksar Fasaee, M. A., Alghamdi, F., Mahinthaku-  
851 mar, K., Berglund, E., and Cominola, A. (2020). “A high-resolution pressure-driven  
852 method for leakage identification and localization in water distribution networks.” *Zenodo*,  
853 <10.5281/zenodo.3924632> (June).

854 Eliades, D. G., Kyriakou, M., Vrachimis, S., and Polycarpou, M. M. (2016). “Epanet-matlab  
855 toolkit: An open-source software for interfacing epanet with matlab.” *Proc. 14th International  
856 Conference on Computing and Control for the Water Industry (CCWI)*, The Netherlands, 8  
857 (Nov).

858 Eliades, D. G. and Polycarpou, M. M. (2012). “Leakage fault detection in district metered areas of

859 water distribution systems.” *Journal of Hydroinformatics*, 14(4), 992–1005.

860 Farley, B., Mounce, S. R., and Boxall, J. B. (2010). “Field testing of an optimal sensor placement  
861 methodology for event detection in an urban water distribution network.” *Urban Water Journal*,  
862 7(6), 345–356.

863 Goulet, J.-a., Coutu, S., and Smith, I. F. (2013). “Model falsification diagnosis and sensor placement  
864 for leak detection in pressurized pipe networks.” *Advanced Engineering Informatics*, 27(2), 261–  
865 269.

866 Greyvenstein, B. and van Zyl, J. E. (2007). “An experimental investigation into the pressure  
867 - leakage relationship of some failed water pipes.” *Journal of Water Supply: Research and*  
868 *Technology-Aqua*, 56(2), 117–124.

869 Huang, L., Du, K., Guan, M., Huang, W., Song, Z., and Wang, Q. (2022). “Combined Usage of  
870 Hydraulic Model Calibration Residuals and Improved Vector Angle Method for Burst Detection  
871 and Localization in Water Distribution Systems.” *Journal of Water Resources Planning and*  
872 *Management*, 148(7), 04022034.

873 Huang, L., Du, K., Guan, M., and Wang, Q. (2020). “The combined usage of the hydraulic model  
874 calibration residual and an improved vectorial angle method for solving the BattLeDIM problem.”  
875 *Zenodo*, <10.5281/zenodo.3925507> (June).

876 Kabaasha, A. M., van Zyl, J. E., and Mahinthakumar, G. K. (2020). “Correcting Power Leakage  
877 Equation for Improved Leakage Modeling and Detection.” *Journal of Water Resources Planning*  
878 *and Management*, 146(3), 06020001.

879 Klise, K. A., Bynum, M., Moriarty, D., and Murray, R. (2017). “A software framework for assessing  
880 the resilience of drinking water systems to disasters with an example earthquake case study.”  
881 *Environmental Modelling & Software*, 95, 420–431.

882 Lambert, A. (1994). “Accounting for Losses: The Bursts and Background Concept.” *Water and*  
883 *Environment Journal*, 8(2), 205–214.

884 Lambert, A. (2001). “What do we know about pressure: Leakage relationships in distribution  
885 systems?.” *Proc. IWA Syst. Approach to Leakage Control Water Distrib. Syst. Manag.*, 8.

886 Li, R., Huang, H., Xin, K., and Tao, T. (2015). “A review of methods for burst/leakage detection  
887 and location in water distribution systems.” *Water Science and Technology: Water Supply*, 15(3),  
888 429–441.

889 Li, Z. and Xin, K. (2020). “Fast localization of multiple leaks in water distribution network jointly  
890 driven by simulation and machine learning.” *Zenodo*, <10.5281/zenodo.3911045> (June).

891 Liemberger, R. and Wyatt, A. (2019). “Quantifying the global non-revenue water problem.” *Water  
892 Supply*, 19(3), 831–837.

893 Liu, R., Zhang, Z., and Zhang, D. (2020). “Leakage detection and isolation in water distri-  
894 bution network based on data mining and genetic optimized hydraulic simulation.” *Zenodo*,  
895 <10.5281/zenodo.3911523> (June).

896 Marzola, I., Mazzoni, F., Alvisi, S., and Franchini, M. (2020). “A pragmatic approach for leak-  
897 age detection based on the analysis of observed data and hydraulic simulations.” *Zenodo*,  
898 <10.5281/zenodo.3900989> (June).

899 Marzola, I., Mazzoni, F., Alvisi, S., and Franchini, M. (2022). “Leakage Detection and Localization  
900 in a Water Distribution Network through Comparison of Observed and Simulated Pressure Data.”  
901 *Journal of Water Resources Planning and Management*, 148(1), 04021096.

902 Min, K. W., Kim, T., Choi, Y. H., Jung, D., and Kim, J. H. (2020). “A two-phase model to detect  
903 and localize water distribution system leakages.” *Zenodo*, <10.5281/zenodo.3922019> (June).

904 Mounce, S., Day, A., Wood, A., Khan, A., Widdop, P., and Machell, J. (2002). “A neural network  
905 approach to burst detection.” *Water Science and Technology*, 45(4-5), 237–246.

906 Mounce, S. R., Boxall, J. B., and Machell, J. (2010). “Development and verification of an online  
907 artificial intelligence system for detection of bursts and other abnormal flows.” *Journal of Water  
908 Resources Planning and Management*, 136(3), 309–318.

909 Pérez, R., Puig, V., Pascual, J., Quevedo, J., Landeros, E., and Peralta, A. (2011). “Methodology  
910 for leakage isolation using pressure sensitivity analysis in water distribution networks.” *Control  
911 Engineering Practice*, 19(10), 1157–1167.

912 Perez, R., Sanz, G., Puig, V., Quevedo, J., Cuguero Escofet, M. A., Nejjari, F., Meseguer, J.,

913 Cembrano, G., Mirats Tur, J. M., and Sarrate, R. (2014). “Leak localization in water networks: A  
914 model-based methodology using pressure sensors applied to a real network in barcelona.” *IEEE*  
915 *Control Systems*, 34(4), 24–36.

916 Pudar, R. S. and Liggett, J. A. (1992). “Leaks in pipe networks.” *Journal of Hydraulic Engineering*,  
917 118(7), 1031–1046.

918 QGIS.org (2020). “QGIS Geographic Information System, <<http://www.qgis.org>>.

919 Romero, L., Blesa, J., Alves, D., Cembrano, G., Puig, V., and Duviella, E. (2020). “Leak local-  
920 ization in water distribution networks using data-driven and model-based approaches.” *Zenodo*,  
921 <10.5281/zenodo.3923501> (June).

922 Romero-Ben, L., Alves, D., Blesa, J., Cembrano, G., Puig, V., and Duviella, E. (2022). “Leak  
923 Localization in Water Distribution Networks Using Data-Driven and Model-Based Approaches.”  
924 *Journal of Water Resources Planning and Management*, 148(5), 04022016.

925 Saldarriaga, J., Solarte, L., Salcedo, C., Montes, C., Martínez, L., González, M., Cuello, M.,  
926 Ariza, A., Galindo, C., Ortiz, N., Gómez, C., and Vanegas, S. (2020). “Battle of the leakage  
927 detection and isolation methods: An energy method analysis using genetic algorithms.” *Zenodo*,  
928 <10.5281/zenodo.3923227> (June).

929 Soldevila, A., Blesa, J., Tornil-sin, S., Duviella, E., Fernandez-canti, R. M., and Puig, V. (2016).  
930 “Leak localization in water distribution networks using a mixed model-based/data-driven ap-  
931 proach.” *Control Engineering Practice*, 55, 162–173.

932 Sophocleous, S., Savić, D., and Kapelan, Z. (2019). “Leak Localization in a Real Water Distri-  
933 bution Network Based on Search-Space Reduction.” *Journal of Water Resources Planning and*  
934 *Management*, 145(7), 04019024.

935 Steffelbauer, D. B., Deuerlein, J., Gilbert, D., Abraham, E., and Piller, O. (2022). “Pressure-Leak  
936 Duality for Leak Detection and Localization in Water Distribution Systems.” *Journal of Water*  
937 *Resources Planning and Management*, 148(3), 04021106.

938 Steffelbauer, D. B., Deuerlein, J., Gilbert, D., Piller, O., and Abraham, E. (2020). “A dual model  
939 for leak detection and localization.” *Zenodo*, <10.5281/zenodo.3923907> (June).

940 Tan, C. A., Phipatanasuphorn, V., and Lai, C. H. A. (2020). “Deep learning of complex pipe leakages  
941 events in drinking water distribution networks for effective spatiotemporal pre-detections and  
942 isolations of leak conditions.” *Zenodo*, <10.5281/zenodo.3902945> (June).

943 Taormina, R., Galelli, S., Tippenhauer, N. O., Salomons, E., Ostfeld, A., Eliades, D. G., Aghashahi,  
944 M., Sundararajan, R., Pourahmadi, M., Banks, M. K., Brentan, B. M., Campbell, E., Lima, G.,  
945 Manzi, D., Ayala-cabrera, D., Herrera, M., Montalvo, I., Izquierdo, J., Luvizotto, E., Chandy,  
946 S. E., Rasekh, A., Barker, Z. A., Campbell, B., Shafiee, M. E., Giacomoni, M., Gatsis, N., Taha,  
947 A., Abokifa, A. A., Haddad, K., Lo, C. S., Biswas, P., Pasha, M. F. K., Kc, B., Somasundaram,  
948 S. L., Housh, M., and Ohar, Z. (2018). “Battle of the Attack Detection Algorithms: Disclosing  
949 Cyber Attacks on Water Distribution Networks.” *Journal of Water Resources Planning and  
950 Management*, 144(8), 04018048.

951 van Zyl, J. E., Lambert, A. O., Collins, R., Zyl, J. E. V., Ph, D., Asce, M., Lambert, A. O.,  
952 Collins, R., and Ph, D. (2017). “Realistic Modeling of Leakage and Intrusion Flows through  
953 Leak Openings in Pipes.” *Journal of Hydraulic Engineering*, 143(9), 04017030.

954 Vrachimis, S. G., Eliades, D. G., and Polycarpou, M. M. (2018a). “Leak detection in water  
955 distribution systems using hydraulic interval state estimation.” *2018 IEEE Conference on Control  
956 Technology and Applications (CCTA)*, IEEE, 565–570 (aug).

957 Vrachimis, S. G., Eliades, D. G., and Polycarpou, M. M. (2018b). “Real-time hydraulic interval  
958 state estimation for water transport networks: a case study.” *Drinking Water Engineering and  
959 Science*, 11(1), 19–24.

960 Vrachimis, S. G., Kyriakou, M. S., Eliades, D. G., and Polycarpou, M. M. (2018c). “LeakDB: A  
961 benchmark dataset for leakage diagnosis in water distribution networks Description of Bench-  
962 mark.” *WDSA / CCWI Joint Conference Proceedings*, Vol. 1 (7).

963 Vrachimis, S. G., Timotheou, S., Eliades, D. G., and Polycarpou, M. M. (2019). “Iterative hydraulic  
964 interval state estimation for water distribution networks.” *Journal of Water Resources Planning  
965 and Management*, 145(1), 04018087.

966 Vrachimis, S. G., Timotheou, S., Eliades, D. G., and Polycarpou, M. M. (2021). “Leakage detec-

967 tion and localization in water distribution systems: A model invalidation approach.” *Control*  
968 *Engineering Practice*, 110, 104755.

969 Wang, X., Li, J., Liu, S., Yu, X., and Ma, Z. (2022). “Multiple Leakage Detection and Isolation in  
970 District Metering Areas Using a Multistage Approach.” *Journal of Water Resources Planning*  
971 *and Management*, 148(6), 04022021.

972 Wang, X., Li, J., Yu, X., Ma, Z., and Huang, Y. (2020). “A multistage approach to detect and  
973 isolate multiple leakages in district metering areas in water distribution systems.” *Zenodo*,  
974 <10.5281/zenodo.3924109> (June).

975 Wu, Y. and Liu, S. (2017). “A review of data-driven approaches for burst detection in water  
976 distribution systems.” *Urban Water Journal*, 14(9), 972–983.

977 Wu, Z. Y. and He, Y. (2020). “Decomposition-based data analysis with hydraulic model calibration  
978 for leakage detection and isolation.” *Zenodo*, <10.5281/zenodo.3908525> (June).

979 Wu, Z. Y. and He, Y. (2021). “Time Series Data Decomposition-Based Anomaly Detection and  
980 Evaluation Framework for Operational Management of Smart Water Grid.” *Journal of Water*  
981 *Resources Planning and Management*, 147(9), 04021059.

982 Wu, Z. Y., Sage, P., and Turtle, D. (2009). “Pressure-Dependent Leak Detection Model and Its  
983 Application to a District Water System.” *Journal of Water Resources Planning and Management*,  
984 136(1), 116–128.

985 Zaman, D., Tiwari, M. K., Gupta, A. K., and Sen, D. (2019). “A review of leakage detection  
986 strategies for pressurised pipeline in steady-state.” *Engineering Failure Analysis*, 104264.

987 Zhang, w., Liu, j., Han, l., Li, y., Li, x., Shi, z., Yu, j., and Wang, j. (2020). “A real time method to  
988 detect the burst location of urban water supply network.” *Zenodo*, <10.5281/zenodo.3923929>  
989 (June).

990 **List of Tables**

991 1 Summary of the different approaches used by the competing teams, at each stage  
992 of their proposed leakage diagnosis methodologies (D: used during detection, L:  
993 used during localization, C: used for calibration, Y: used in general). . . . . 40  
994 2 Explanation of features included in the methodologies of the competing teams. . . 41  
995 3 Parameters used in the evaluation procedure. . . . . 42  
996 4 BattLeDIM competition results and ranking of top 6 participating teams. . . . . 43

FEATURE	Cheng00	DandW	Leak-busters	CIA- CUA	Tsing-hua	Under- Pressure	Zhiyun Shuiwu	IRI	KU Hydro- systems	Infra- Sense Labs	DHI China	Tongji	Wu BSY	Cuba- lytics	Arte- sia	DHI Singa- pore	UNIFE	Flu- Ing
Use nominal model	D	D	D	D	D	DL	DL	L	L	L	L	L	L	L	L	D	CDL	CL
Model calibration				Y	Y	Y	Y	Y	Y	Y	Y	Y	Y	Y	Y	Y	Y	Y
AMR based demands				C	C	C	C	C	C	Y	Y	Y	Y	Y	Y	Y	Y	Y
Normal operation dataset and/or dual model	D	D	D	D	D	DL				Y	Y	Y	Y					D
Areas treated differently	Y	Y					Y	Y										Y
Pressure Sensitivity Matrix		DL				L												
Pressure reconstruction/comparison	L						DL								L			
Residuals - Model-based	D	DL	D	D	DL		DL	L	L	L	DL	DL	D					D
Residuals - Model-free			D				DL	DL	D						D			
Change Detection	D	L	D	D	DL	D	D	L				D	D					D
Time Series Analysis/Signal Processing/EMD				DL	DL	DL						D	D					D
Statistical Methods	L	D											D					D
Machine Learning and Soft Computing				D							D				D	DL		
Simulation-based optimization			L	L	L		L	L			L	L	L	L	L	C	CL	CL
Simulating leaks			L	L	L		L	L	L	L	L	L	L	L	L	C		
Mathematical Programming			L						L			C						
Meta-heuristics			L	L	D	DL	DL	C	CL							C		CL
Ad-hoc/Engineering judgement													DL	D	DL			DL

**TABLE 1.** Summary of the different approaches used by the competing teams, at each stage of their proposed leakage diagnosis methodologies (D: used during detection, L: used during localization, C: used for calibration, Y: used in general).



FEATURE	DESCRIPTION
Use nominal model	Making use of the provided EPANET model for L-Town
Model calibration	Nominal model calibration of demands and/or pipe parameters
AMR based demands	Use of AMR data to model demand patterns
Normal operation dataset and/or dual model	Use of a (calibrated) EPANET model to create dataset under normal operations (no leak) and/or a normal operation model
Areas treated differently	Whether the algorithms treat different areas of the network separately
Pressure Sensitivity Matrix	Linearization of hydraulic equations
Pressure reconstruction/comparison	Reconstruction/comparison of pressure of neighboring nodes
Residuals - Model-based	Residuals computed between simulated readings from available nominal model simulations and observed SCADA
Residuals - Model-free	Residuals computed between predicted readings from model-free approach and observed SCADA
Change Detection	Technique to identify abrupt change in residuals/observations in time (CUSUM, angle method)
Time Series Analysis/Signal Processing/EMD	Methods pertaining to TSA/SP such as Empirical Model Decomposition, spectral methods used at different stages of the algorithm
Statistical Methods	Methods based on comparison with statistical distribution of the observed data, hypothesis testing, linear regression, etc.
Machine Learning and Soft Computing	Includes supervised/unsupervised machine learning (also feature engineering), fuzzy methods
Simulation-based optimization	Use of an optimization method with objective function based on simulation via hydraulic model
Simulating leaks	Use of an EPANET model to simulate leaks
Mathematical Programming	Methods including Integer Programming, Dynamic Programming, Mixed Integer Programming
Meta-heuristics	Global optimization methods such as Genetic Algorithms, Harmony Search and Particle Swarm Optimization
Ad-hoc/Engineering judgement	Techniques that cannot be framed in the methods above or methods based on engineering common sense

**TABLE 2.** Explanation of features included in the methodologies of the competing teams.

Parameter	Value	Description
$x_{max}$	300 (Meters)	Maximum detection radius
$c_w$	0.80 (Euro)	Cost of water per $m^3$
$c_r$	500 (Euro)	Maximum repair crew cost

**TABLE 3.** Parameters used in the evaluation procedure.

Team Name (Label)	Pareto Rank	True Positive Rate	False Positives Count	Economic Score (Euro)
Tongji-Team (L)	1	56.52%	3	€264,873
Under Pressure (O)	1	65.22%	4	€260,562
IRI (H)	2	43.47%	1	€210,772
Leakbusters (K)	2	47.83%	7	€195,490
Tsinghua (M)	3	47.83%	5	€167,981
UNIFE (N)	4	43.47%	4	€127,626
PERFECT	-	100%	0	€523,154

**TABLE 4.** BattLeDIM competition results and ranking of top 6 participating teams.

997 **List of Figures**

998 1 The L-Town Benchmark Network. . . . . 45

999 2 Demand signal decomposition using Fourier Series. . . . . 46

1000 3 Location of pressure sensors in the L-Town network. . . . . 47

1001 4 Location of AMRs (nodes with red colour) in “Area C” of the L-Town network. . . 48

1002 5 Location of leakages in 2018 dataset. . . . . 49

1003 6 Location of leakages in 2019 dataset. . . . . 50

1004 7 Evolution of leakages in 2019 dataset. . . . . 51

1005 8 Example of the scoring function for a true detection:  $q(k) = 100 \text{ m}^3/h$  (leakage  
1006 flow),  $c_w = 1 \text{ euro/m}^3$  (water cost),  $c_r = 500 \text{ euro/detection}$  (max crew cost) . . . . 52

1007 9 Total volume of water lost from each leakage in the BattLeDIM problem, sorted  
1008 chronologically and identified by the corresponding link ID. . . . . 53

1009 10 (a) Final scores of the BattLeDIM competition: Team rankings are based only on  
1010 the *Economic score*. The ‘Perfect’ score is the theoretical upper bound; (b) Team  
1011 scores with respect to the *True Positive Rate* metric; (c) Team scores with respect  
1012 to the number of *False Positives*. . . . . 54

1013 11 Multi-parameter score (Economic score and True Positive Rate) of the submitted  
1014 results. The best scores are in the upper-right corner of the graph. . . . . 55

1015 12 Sensitivity analysis of the Economic score with respect to the price of water: (a)  
1016 0.40, (b) 0.60, (c) 0.80, (d) 1.00, (e) 1.20 Euro. Note that the True Positive Rates  
1017 (TPR) and number of False Positives (FP) remain the same in these scenarios. . . . 56

1018 13 (a) Alternative *Economic Score* and ranking of teams in the BattLeDIM competition  
1019 using the alternative evaluation criteria in which the leakage volume is normalized;  
1020 (b) *True Positive Rate* score; (c) Number of False positives. . . . . 57

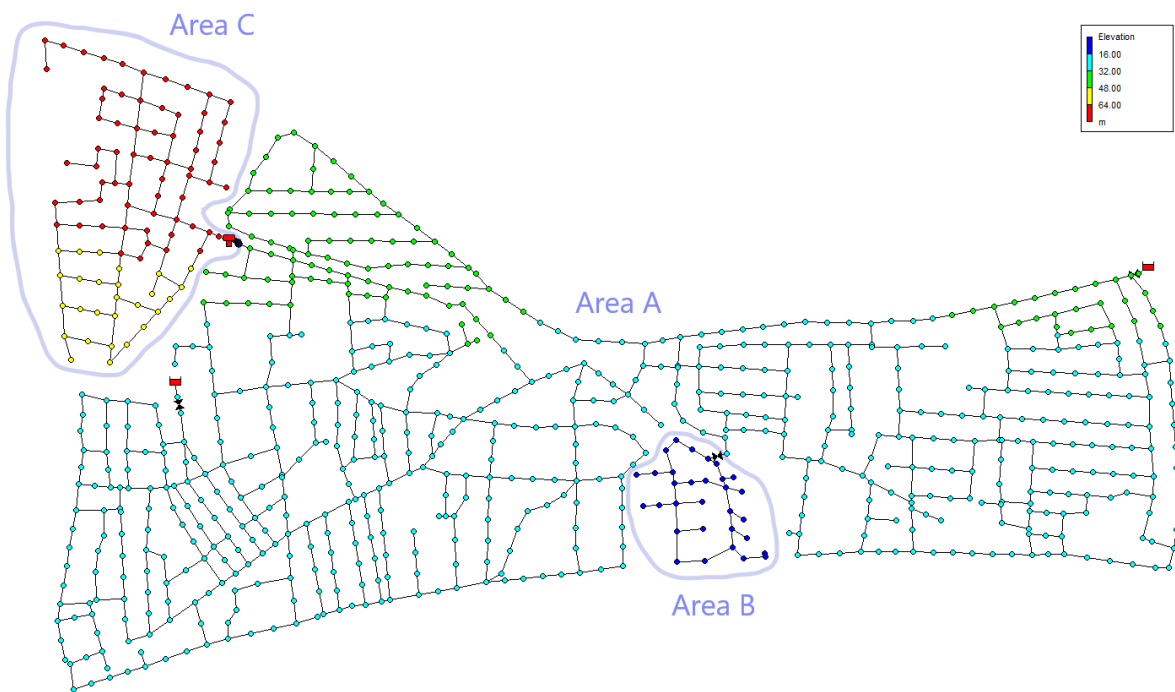


**Fig. 1.** The L-Town Benchmark Network.

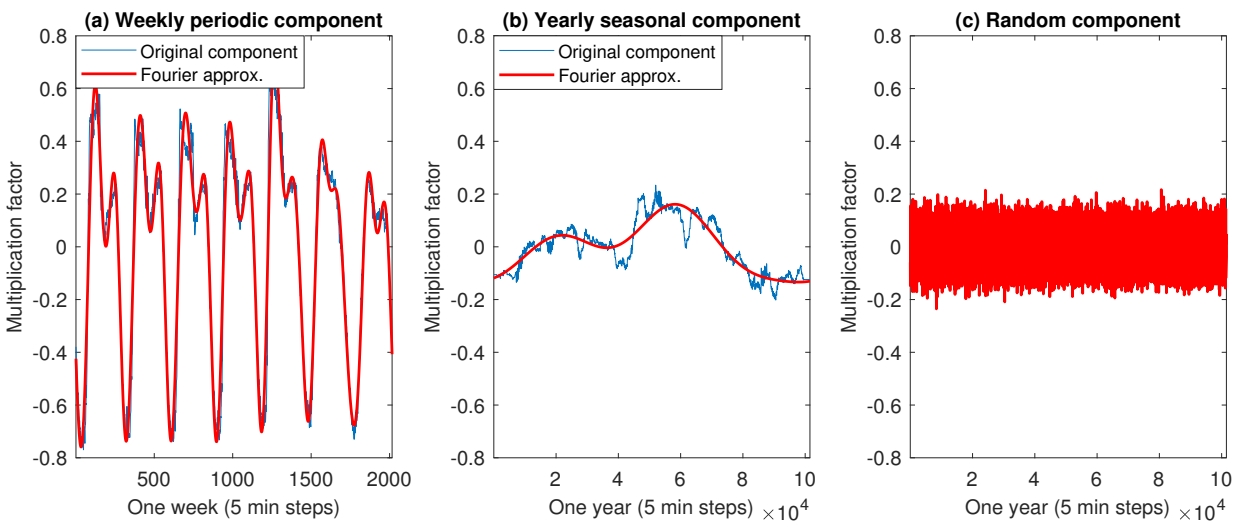


**Fig. 2.** Demand signal decomposition using Fourier Series.

Pressure Sensors (33)

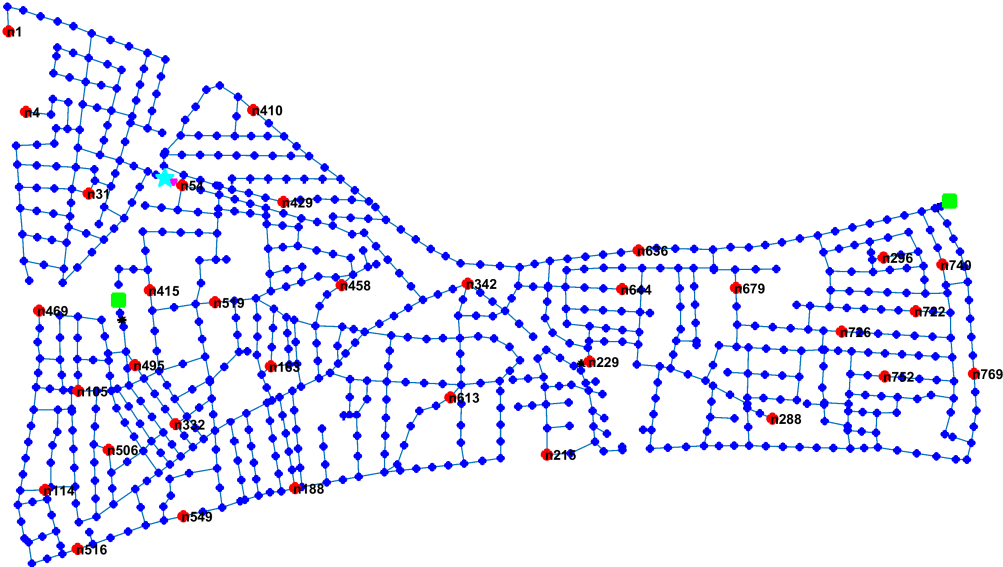
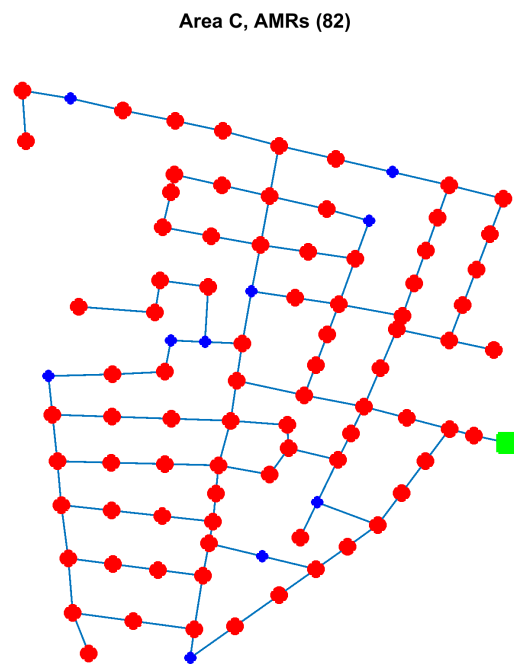
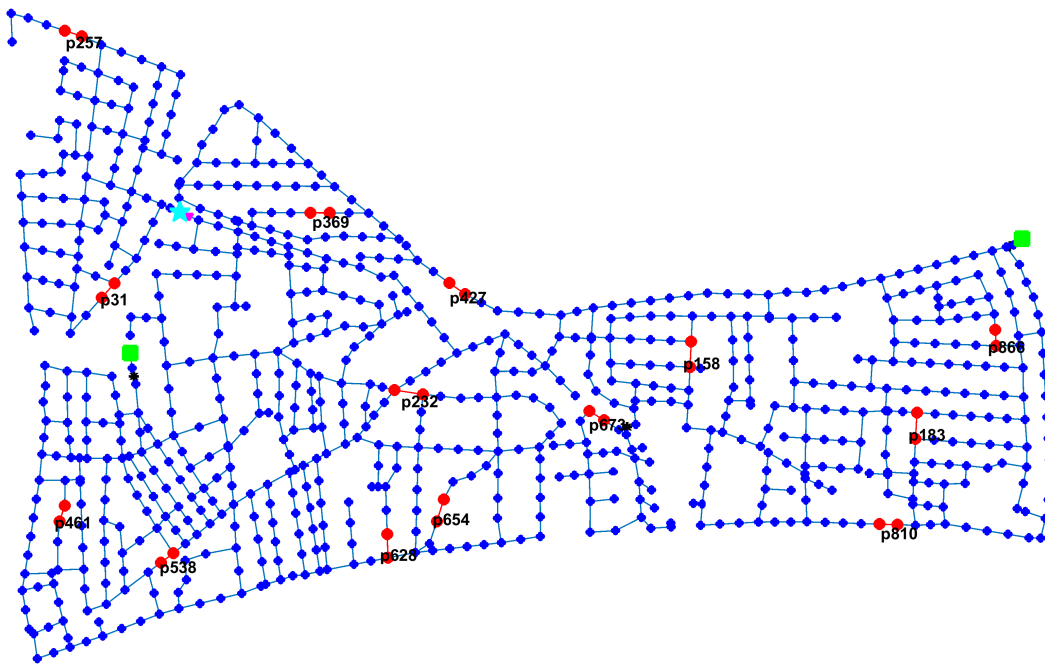


Fig. 3. Location of pressure sensors in the L-Town network.



**Fig. 4.** Location of AMRs (nodes with red colour) in “Area C” of the L-Town network.





**Fig. 5.** Location of leakages in 2018 dataset.

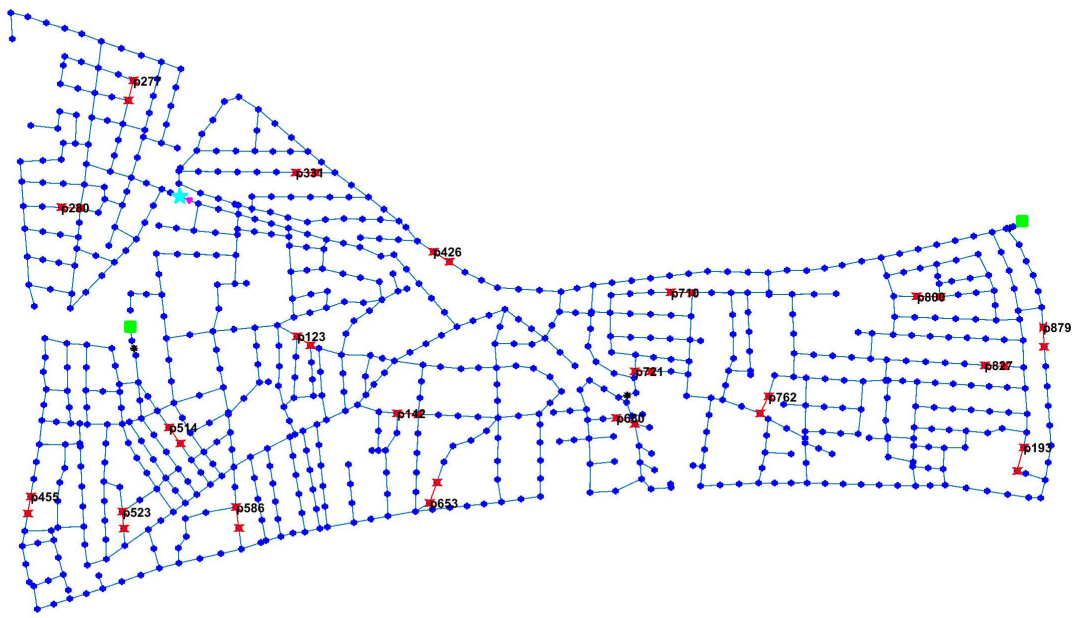


**Fig. 6.** Location of leakages in 2019 dataset.

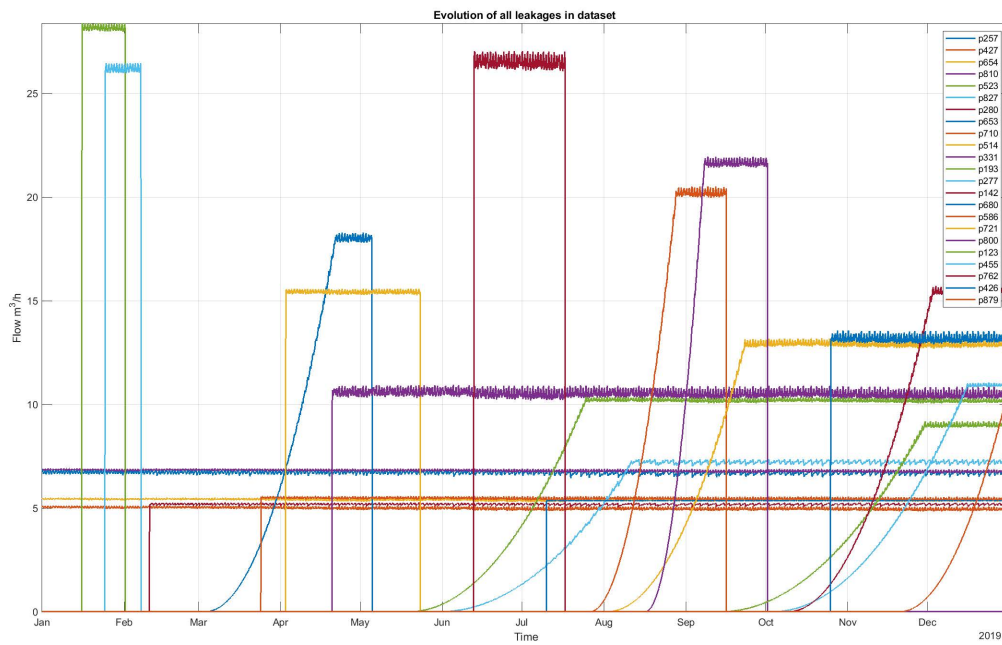


**Fig. 7.** Evolution of leakages in 2019 dataset.

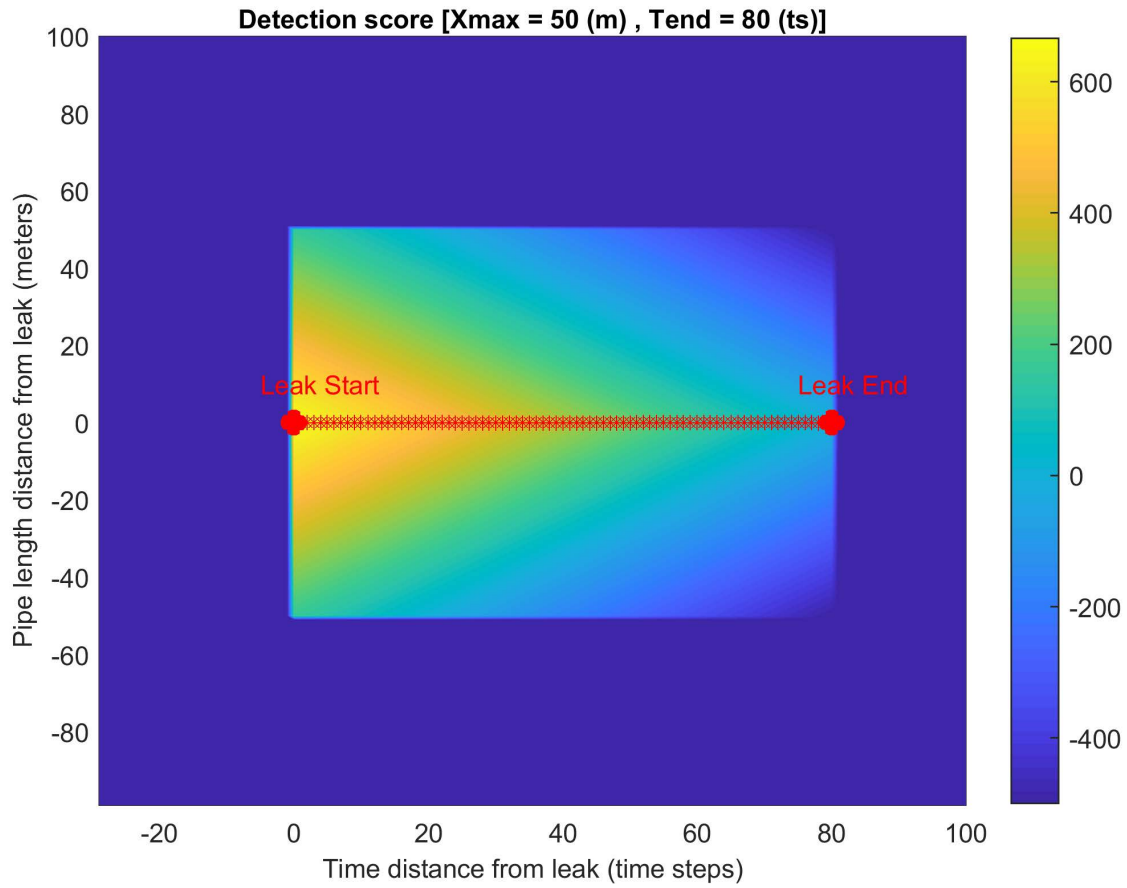


**Fig. 8.** Example of the scoring function for a true detection:  $q(k) = 100 \text{ m}^3/\text{h}$  (leakage flow),  $c_w = 1 \text{ euro}/\text{m}^3$  (water cost),  $c_r = 500 \text{ euro}/\text{detection}$  (max crew cost)

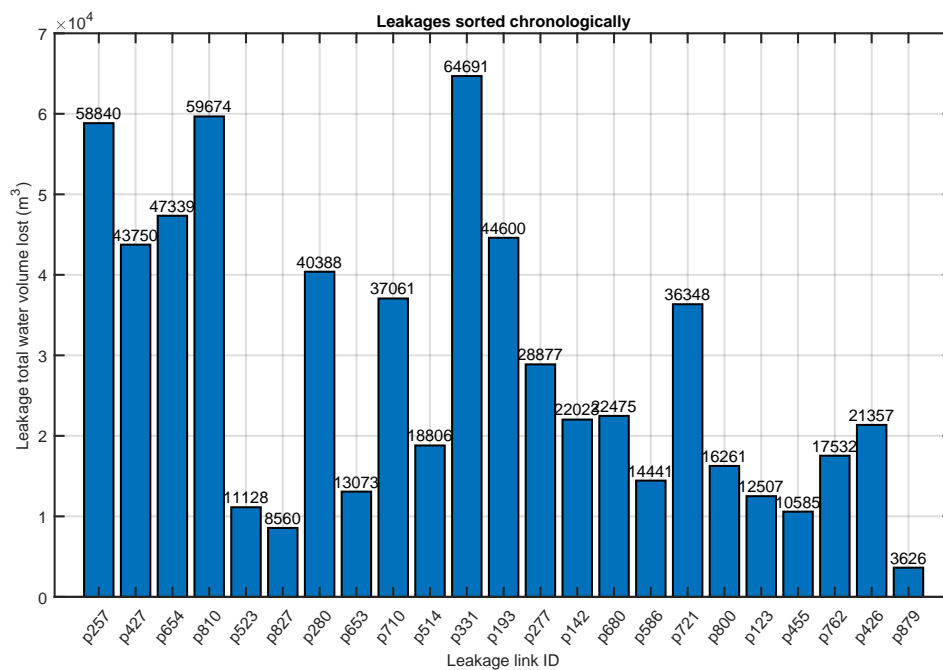


**Fig. 9.** Total volume of water lost from each leakage in the BattLeDIM problem, sorted chronologically and identified by the corresponding link ID.

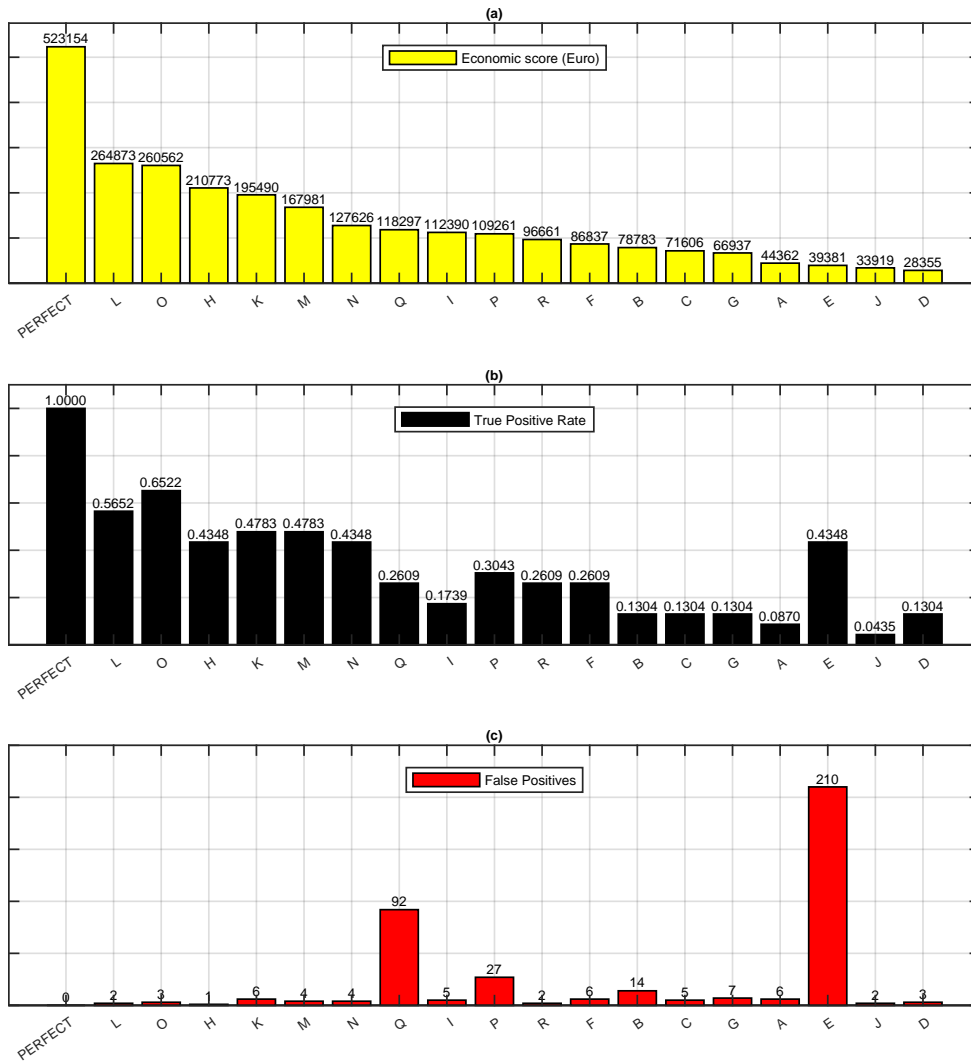


**Fig. 10.** (a) Final scores of the BattLeDIM competition: Team rankings are based only on the *Economic score*. The ‘Perfect’ score is the theoretical upper bound; (b) Team scores with respect to the *True Positive Rate* metric; (c) Team scores with respect to the number of *False Positives*.

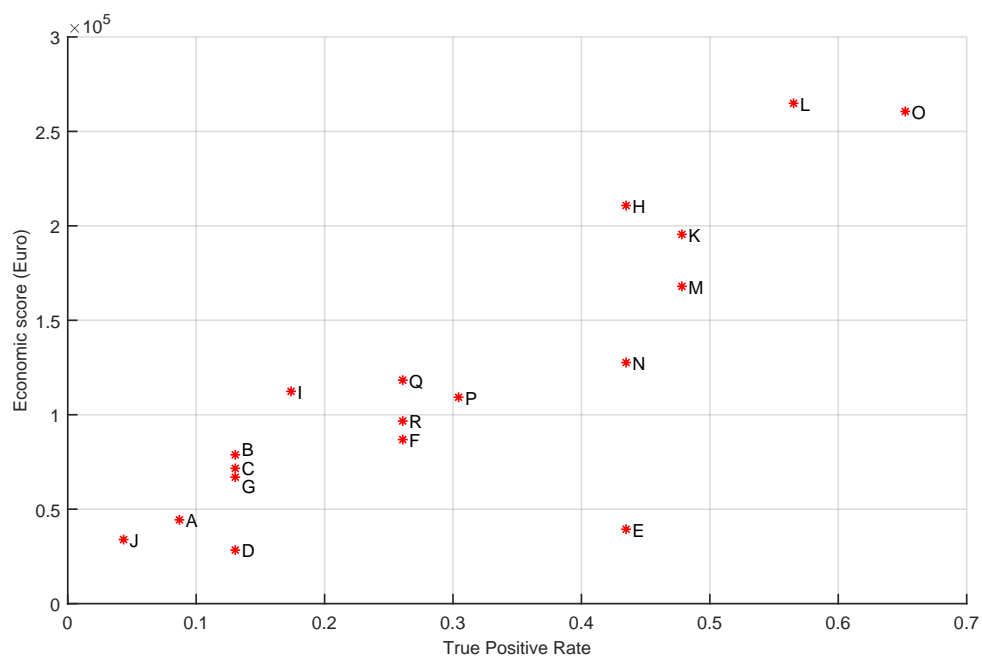


**Fig. 11.** Multi-parameter score (Economic score and True Positive Rate) of the submitted results. The best scores are in the upper-right corner of the graph.

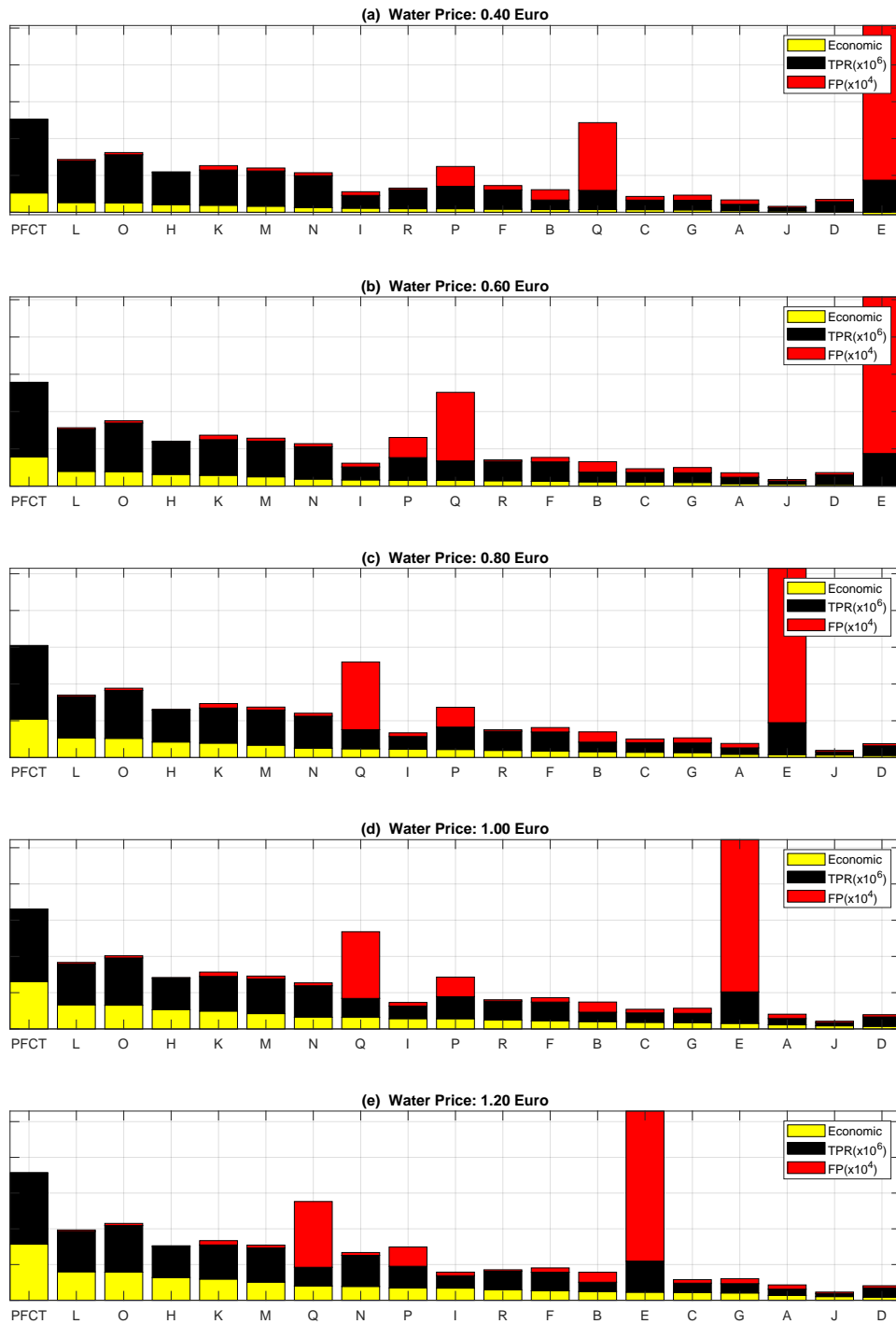


**Fig. 12.** Sensitivity analysis of the Economic score with respect to the price of water: (a) 0.40, (b) 0.60, (c) 0.80, (d) 1.00, (e) 1.20 Euro. Note that the True Positive Rates (TPR) and number of False Positives (FP) remain the same in these scenarios.



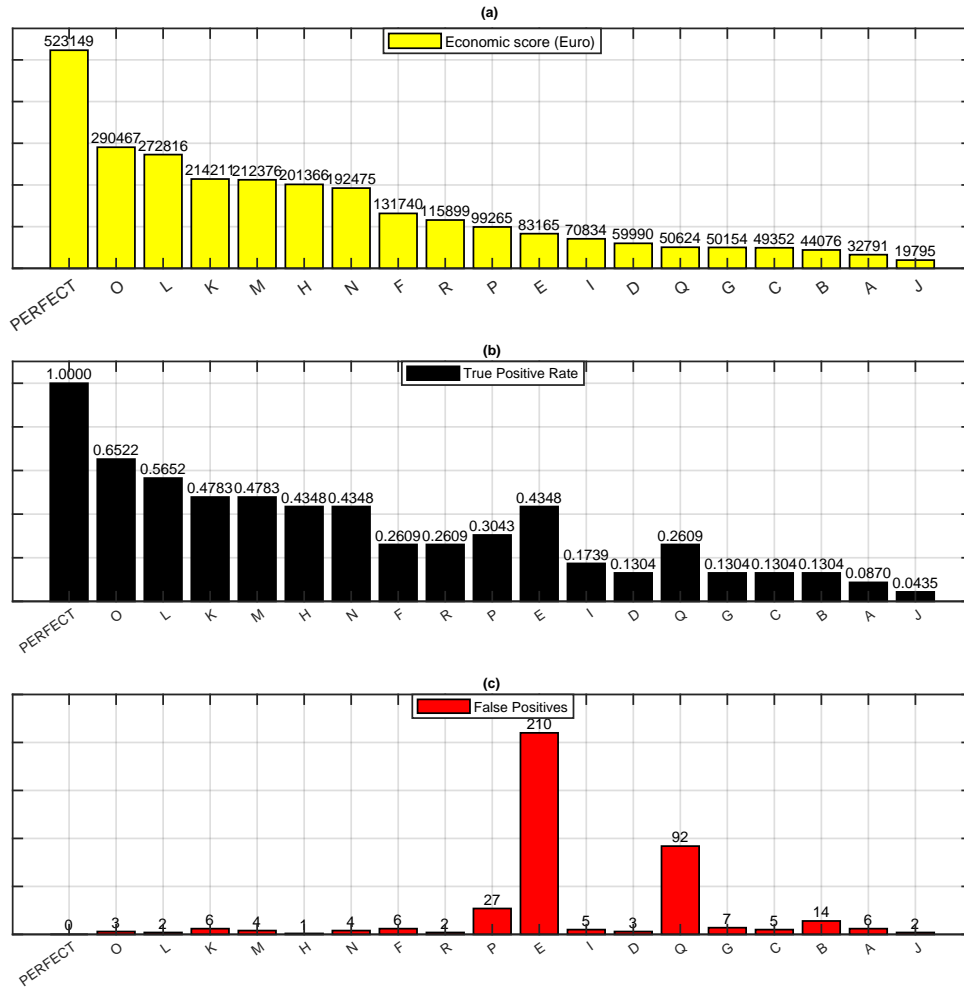


**Fig. 13.** (a) Alternative *Economic Score* and ranking of teams in the BattLeDIM competition using the alternative evaluation criteria in which the leakage volume is normalized; (b) *True Positive Rate* score; (c) Number of False positives.